From the DIVISION OF INTEGRATIVE PHYSIOLOGY
DEPARTMENT OF PHYSIOLOGY AND PHARMACOLOGY
Karolinska Institutet, Stockholm, Sweden

SKELETAL MUSCLE PLASTICITY AND ENERGY METABOLISM

LEONIDAS S. LUNDELL

Karolinska Institutet

Stockholm 2017

Published by Karolinska Institutet.
Printed by E-Print AB

ISBN 978-91-7676-909-6

SKELETAL MUSCLE PLASTICITY AND ENERGY METABOLISM

THESIS FOR DOCTORAL DEGREE (Ph.D.)

By

Leonidas S. Lundell

Defended on

Friday the 15th of December, 2017, 9:00 am,
Gard aula, Nobels väg 18, Solna

Principal Supervisor:
Professor Juleen R. Zierath
Karolinska Institutet
Department of Physiology and Pharmacology
and
Department of Molecular Medicine and Surgery
Division of Integrative Physiology

Co-supervisor(s):
Professor Anna Krook
Karolinska Instituet
Department of Physiology and Pharmacology
and
Department of Molecular Medicine and Surgery
Division of Integrative Physiology

Associate Professor Alexander V. Chibalin
Karolinska Institutet
Department of Molecular Medicine and Surgery
Division of Integrative Physiology

Opponent:
Professor Francesco Giorgino
University of Bari Aldo Moro
Department of Emergency and Organ Transplants

Examination Board:
Professor Michael Kjaer
Copenhagen University Hospital
Department of Clinical Medicine

Professor Eva Blomstrand
Swedish School of Sport and Health Sciences
Department of Performance and Training

Professor Lars Larsson
Karolinska Institutet,
Department of Physiology and Pharmacology

When I heard the learn’d astronomer,

When the proofs, the figures, were ranged in columns before me,

When I was shown the charts and diagrams, to add, divide, and measure them,

When I sitting heard the astronomer where he lectured with much applause in the lecture-room,

How soon unaccountable I became tired and sick,

Till rising and gliding out I wander’d off by myself,

In the mystical moist night-air, and from time to time,

Look’d up in perfect silence at the stars.

Walt Whitman

ABSTRACT

Skeletal muscle is remarkable in its ability to adjust to our needs. It can change its energy stores and usage, as well as its total mass. Furthermore, skeletal muscle adapts to deactivate reactive oxygen species produced, which in turn can both damage cells and convey signals. The molecular mechanisms regulating skeletal muscle plasticity are many, including reactive oxygen species, AMPK, and FOXO. AMPK functions as a molecular energy sensor, while the FOXO proteins are transcription factors that bind to the DNA, and regulate gene transcription.

To understand the role of reactive oxygen species in health, we investigated how an intravenous antioxidant infusion of N-acetyl-cysteine (NAC), affected exercise-modulated insulin sensitivity. We found that NAC infusion decreased whole-body insulin sensitivity and skeletal muscle p70S6K phosphorylation, indicating diminished glucose uptake and attenuated protein synthesis.

We also investigated the changes occurring in the atrophying skeletal muscle of individuals with spinal cord injury. We find that AMPK signaling decreases during the first year after injury, and that protein content of the AMPK regulatory γ1 subunit decreased, and γ3 increased. Skeletal muscle energy metabolism decreased during the first year after spinal cord injury, as indicated by the decreased protein content of the mitochondrial respiration complexes I-III. The contractile myosin heavy chain proteins myosin heavy chain 1 declined, and myosin heavy chain IIa increased 12 months after spinal cord injury.

In order to understand how the changes in energy metabolizing and contractile proteins occurred, we investigated the mechanisms mediating protein degradation and synthesis, namely translation, autophagy and proteasomal degradation. We found that protein content of LC3II, as well as protein content and phosphorylation of S6 kinase, increased transiently during the first year after injury, indicating a temporary increase in autophagy and protein synthesis. We also detected stably increased levels of Lys48 poly-ubiquitinated proteins, indicating constantly increased proteasomal degradation during the first year after injury.

Additionally, FOXO3 protein content, and FOXO1 phosphorylation decreased during the first year after spinal cord injury. To better understand the metabolic role of FOXO proteins, we transfected mouse skeletal muscle with FOXO proteins modified to bind to the DNA without activating transcription, leading to inhibited expression of FOXO regulated genes. We find that inhibition FOXO transcriptional activity decreased skeletal muscle glucose uptake, and increased inflammatory signaling and immune cell infiltration.

Together, these studies partly elucidate how skeletal muscle adapts to its changing environment. We find that reactive oxygen species appear to be involved in the beneficial effects of exercise, and we unravel the signals and mechanisms mediating decreased skeletal muscle mass after spinal cord injury. Finally, we find that FOXO proteins directly affect gene networks involved in regulating inflammation and glucose metabolism in skeletal muscle.

LIST OF SCIENTIFIC PAPERS

Articles included in this thesis:

Study I:

Trewin AJ, **Lundell LS**, Perry BD, Patil KV, Chibalin AV, Levinger I, McQuade LR, Stepto NK. Effect of N-acetylcysteine infusion on exercise-induced modulation of insulin sensitivity and signaling pathways in human skeletal muscle. Am J Physiol Endocrinol Metab. 2015. 309(4):E388-97

Study II:

Kostovski E, Boon H, Hjeltnes N, **Lundell LS**, Ahlsén M, Chibalin AV, Krook A, Iversen PO, Widegren U. Altered content of AMP-activated protein kinase isoforms in skeletal muscle from spinal cord injured subjects. Am J Physiol Endocrinol Metab. 2013. 305(9):E1071-80

Study III:

Lundell LS, Savikj M, Kostovski E, Iversen PO, Zierath JR, Krook A, Chibalin AV, and Widegren U. Protein translation, proteolysis, and autophagy in human skeletal muscle atrophy after spinal cord injury. Unpublished.

Study IV:

Lundell LS, Massart J, Krook A, Zierath JR. Regulation of Glucose Uptake and Inflammation Markers by FOXO1 and FOXO3 in Skeletal Muscle. Unpublished

Articles not included in this thesis

Pirkmajer S, Kirchner H, **Lundell LS**, Zelenin PV, Zierath JR, Makarova KS, Wolf YI, Chibalin AV. Early vertebrate origin and diversification of small transmembrane regulators of cellular ion transport. J Physiol. 2017. 595(14):4611-4630.

Massart J, Sjögren RJO, **Lundell LS**, Mudry JM, Franck N, O'Gorman DJ, Egan B, Zierath JR, Krook A. Altered miR-29 Expression in Type 2 Diabetes Influences Glucose and Lipid Metabolism in Skeletal Muscle. Diabetes. 2017. 66(7):1807-1818.

CONTENTS

LIST OF ABBREVIATIONS

4E-BP1	Eukaryotic translation initiation factor 4E-binding protein 1
ACC	Acetyl-CoA carboxylase
Akt	RAC-alpha serine/threonine-protein kinase
AMPK	5'-AMP-activated protein kinase
ATP	Adenosine triphosphate
ADP	Adenosine diphosphate
AMP	Adenosine monophosphate
CaMKK β	Calcium/calmodulin-dependent protein kinase kinase beta
CCR7	C-C chemokine receptor type 7
CD36	Fatty acid translocase
CPT1	Carnitine O-palmitoyltransferase 1
FOXO	Forkhead box protein O
GLUT4	Facilitated glucose transporter member 4
GS	Glycogen synthase
GSK	Glycogen synthase kinase
GSH	Glutathione
GSSG	Glutathione disulfide
IGF1	Insulin like growth factor 1
LC3	Microtubule-associated proteins 1A/1B light chain 3B
LKB1	Liver kinase B1
Lys48	Lysine residue 48
Lys63	lysine residue 63
MAFbx	F-box only protein 32
MHC-I	Myosin heavy chain type I
MHC-IIa	Myosin heavy chain type Iia
MHC-IIx	Myosin heavy chain type Iix
mTOR	Mammalian target of rapamycin
mTORC1	mTOR complex 1
mTORC2	mTOR complex 2
MuRF1	Muscle ring finger protein 1
NAC	N-acetyl-cysteine
NADH	Nicotinamide adenine dinucleotide
NADPH	Nicotinamide adenine dinucleotide phosphate
p70S6K	p70 S6 kinase
PDK1	Phosphoinositide-dependent kinase-1
PDK4	Pyruvate dehydrogenase kinase 4
PGC-1α	Peroxisome proliferator-activated receptor γ coactivator 1-α
PI3K	Phosphoinositide 3-kinase
Rheb	Ras homolog enriched in brain
S6	Ribosomal S6 kinase
SOD	Superoxide dismutase
SEM	Standard error of mean
SD	Standard deviation
TBC1D1	TBC1 domain family member 1

TBC1D4	TBC1 domain family member 4
TCA	tricarboxylic acid cycle
TSC1	Tuberous sclerosis 1
TSC2	Tuberous sclerosis 2
ULK	Serine/threonine-protein kinase ULK1

1 INTRODUCTION

Skeletal muscle is a remarkable organ without which metazoan life would be not be recognizable today. The main role of skeletal muscle is locomotion, but its functions span far beyond. It is becoming increasingly clear that it has an essential role as an endocrine organ, both by regulating energy metabolism, and by secreting hormones. Skeletal muscle accounts for approximately 40% of total body mass, consumes about 30% of our basal metabolic rate [1], absorbs ~30% of postprandial glucose [2], while accounting for ~80% of insulin stimulated glucose uptake [3].

Skeletal muscle is a remarkably plastic organ. Exercise can increase muscle mass dramatically, and alters function by changing expression of energy metabolizing enzymes, mitochondrial density, vascularization, and myofiber nucleation. On the other end of the spectrum, inactivity, disease, and spinal cord injury lead to changes in fiber type distribution, and energy metabolizing enzymes in skeletal muscle.

Furthermore, skeletal muscle is a primary site of insulin resistance in people with type 2 diabetes. Loss of skeletal muscle mass (skeletal muscle atrophy) is debilitating both in terms of life quality due to reduced mobility and longevity due to weakened metabolic health. The role of skeletal muscle in endocrine health is manifold. It functions as a storage site for glucose and amino acids, and its storage capacity is vital for buffering energy abundance and shortage. Perturbations in energy storage are one of the root causes of today's global obesity and health crisis. Moreover skeletal muscle functions also as an endocrine organ by secreting systemic and local myokines necessary for whole-body metabolic health.

1.1 SKELETAL MUSCLE STRUCTURE AND METABOLISM.

1.1.1 Structure and fiber types

Skeletal muscle is composed of muscle fibers, with each fiber containing several myofibrils supported by a single muscle cell. The myofibrils are further subdivided into the most basic repeating unit of the skeletal muscle organ: the sarcomere. The sarcomere is defined as the structure between two Z lines, and is the structure responsible for force generation by the sliding of thick myosin filaments across thin actin filaments (reviewed in [4]).

Human skeletal muscle fibers are subcategorized into three types based on their contractile and molecular properties: type I, type IIa, and type IIx fibers. Rodent skeletal muscle fibers have an additional fiber type denoted type IIb. The fiber type classification is based on several parameters including shortening velocity, myosin ATPase activity, or myosin heavy chain composition.

Type I fibers, also called slow-twitch fibers, contract relatively slowly, are slow to fatigue, contain the slow isoform of myosin, myosin heavy chain I (MHC-I), and have a predominantly oxidative metabolism mediated through high mitochondrial density. Furthermore, they demonstrate high insulin sensitivity and high rate of glucose uptake, and are rich in myoglobin giving them a red color.

Type IIa fibers, also called fast-twitch fibers, have intermediate features with both oxidative and glycolytic metabolism. They contract relatively fast, have intermediate fatigue time, and express myosin heavy chain IIa (MHC-IIa). Type IIa fibers are poor in myoglobin giving them a white appearance.

Type IIx, also referred to as fast-twitch fibers, have the fastest contractile speed of all human muscle fibers by expressing myosin heavy chain IIx (MHC-IIx), and their low mitochondrial density leads them to metabolize glucose, predominantly through glycolysis. Furthermore they express low levels of the facilitative glucose transporter subtype 4 (GLUT4) and have the lowest insulin sensitivity. As in the Type IIa fibers they have little myoglobin giving them a light color.

The molecular and phenotypic properties correlate well with the observations that endurance athletes have a higher proportion of oxidative type I fibers and a high rate of whole-body glucose disposal [5], while patients with type 2 diabetes have a relative lower proportion of type I fibers and a relative higher proportion of type IIx fibers, concomitant with an impaired lower whole-body glucose disposal [6, 7]. Furthermore, skeletal muscle plasticity extends to fiber type distribution, and takes different forms depending on the external stimuli. Fasting [8], sepsis [9] and glycocorticoid administration [10] affect mainly slow-twitch fibers, while immobilization [11], unloading (both experimental and through microgravity exposure [12]), and spinal cord injury affect fast-twitch fibers [13].

1.1.2 Whole-body glucose homeostasis

Whole-body glucose homeostasis is mediated through the reciprocal regulatory action of insulin and glucose, as well as glucagon, cortisol and adrenalin. Increased glucose levels in the blood stream lead to increased insulin secretion, which in turn leads to the absorption of glucose into skeletal muscle, liver, and adipose tissue. Insulin has several additional effects, including increased glycogen synthesis in liver and muscle, as well as an anabolic role by increasing protein synthesis. Insulin-induced absorption of blood glucose leads to suppression of insulin secretion from the pancreas due to reduced blood glucose levels.

1.1.3 Glucose uptake

Skeletal muscle glucose uptake is a tightly regulated process. Insulin binding to the insulin receptor leads to phosphorylation of the insulin receptor substrate 1, which recruits and activates phosphoinositide 3 kinase (PI3K) to the cell surface [14]. PI3K recruits both protein kinase B (Akt) and phosphoinositide-dependent kinase-1 (PDK1) [15] to the cell membrane, where PDK1 and mechanistic target of rapamycin (mTOR) complex 2 (mTORC2) phosphorylate Akt on different sites, an activating phosphorylation. Fully activated Akt leads to phosphorylation and inhibition of TBC1 domain family member 4 (TBC1D4) [16] and TBC1D1 [17]. TBC1D1/4 function as GTPase activating proteins (GAP), inhibiting the small monomeric GTP proteins of the Rab and Rac family. GAP inhibition leads to activation of Rab and Rac proteins, and translocation of GLUT4 containing vesicles to the plasma membrane, thereby increasing glucose transport into the cell [18].

In addition to insulin, skeletal muscle contraction by itself increases GLUT4 surface content and glucose uptake. Insulin and muscle contraction induce GLUT4 translocation to the cell membrane by modulating TBC1D1/4 [19]. Furthermore, skeletal muscle contraction increases glucose uptake both independently and synergistically with insulin [20, 21] through the activation of AMP-activated kinase (AMPK) [22] and other mechanisms [23, 24]. The high energy demands of contracting skeletal muscle alter energy balance by increasing both glucose uptake and utilization locally. Systemically, skeletal muscle contraction affects energy homeostasis by mobilizing stored energy depots throughout the body, and stimulating the secretion of myokines that shift homeostasis to the specific organismal needs.

1.1.4 Glucose metabolism

Once glucose is transported across the skeletal muscle cell membrane, it has two major fates depending on the energy status of the myocyte. If energy supply is abundant, glucose enters the glycogenesis pathway and becomes polymerized to glycogen. In situations of energy demand, such as during exercise, glucose will be oxidized. Glucose oxidation is achieved by three interwoven enzymatic processes: glycolysis, the tricarboxylic acid (TCA, also known as Krebs, or citric acid cycle), and oxidative phosphorylation. Together these processes generate ATP and NADH.

Glycolysis, the first step in glucose metabolism, is the least efficient of the three metabolic cascades in terms of ATP production (summarized in figure 1). At the same time, the products of glycolysis are essential for subsequent energy production steps. Glycolytic degradation of glucose is achieved through 10 discrete steps, with hexokinase catalyzing the first (and rate limiting) step, and pyruvate kinase the last step. The Krebs cycle consumes pyruvate generated in glycolysis, and converts it into among other things NADH. Finally the oxidative phosphorylation cascade utilizes the NADH produced in previous steps to generate a proton motive force across the inner mitochondrial membrane. The proton motive force is generated by the shuttling of electrons through complex I-IV, coupled to translocation of H^+ towards

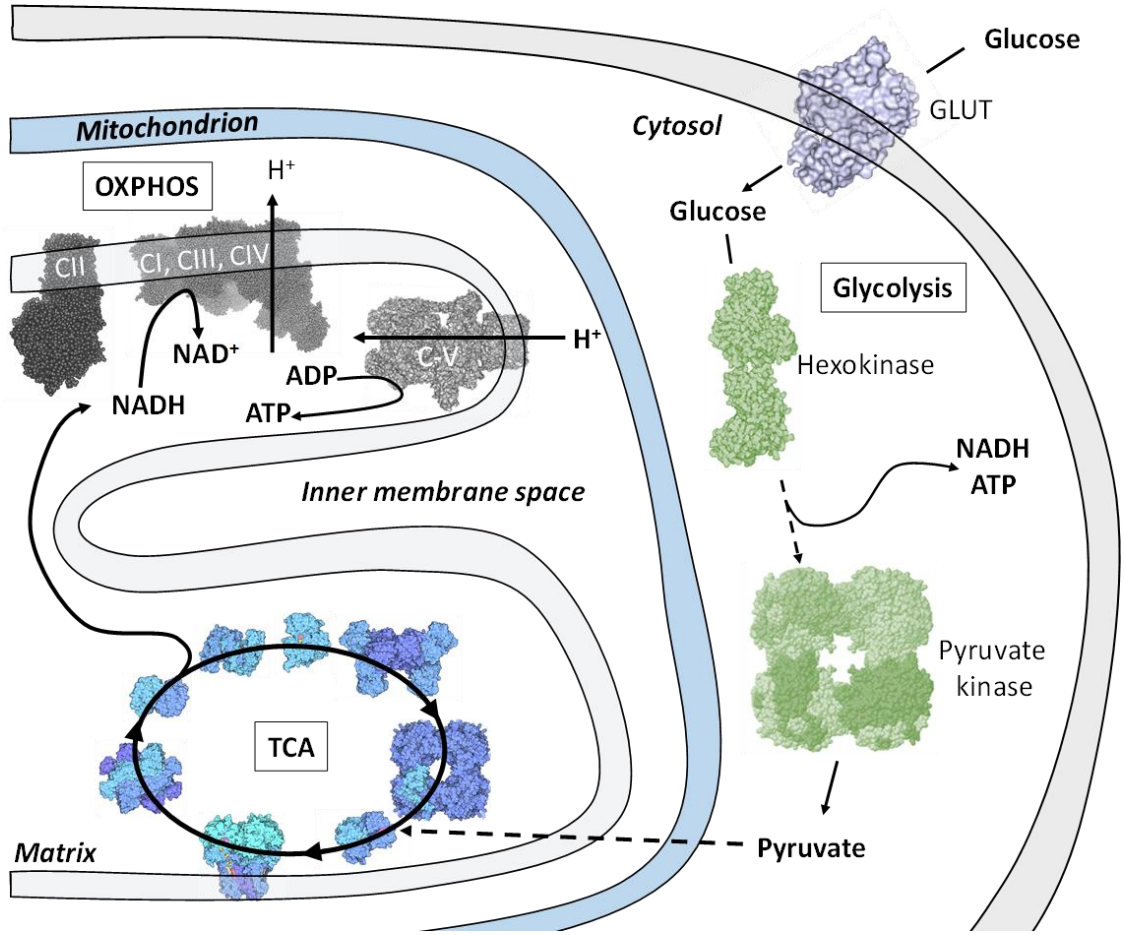

Figure 1. Schematic representation of cellular energy metabolism. Dashed arrow indicates multistep cascade not shown here, molecules are not scale. Glucose is taken up by glucose transporters (GLUT1 as purple enzyme, GLUT4 crystal structure not elucidated), and enters glycolysis (green) which through a multistep pathway generates NADH, ATP and pyruvate. Pyruvate is utilized in the citric acid cycle (TCA, blue) and generate additional NADH. The oxidative phosphorylation enzymes (OXPHOS in gray) generate a proton gradient by consuming NADH in the respirasome (CI, CIII, CIV). The ATPase utilizes the proton gradient to generate ATP from ADP. PDB files to generate figures where: 4pyp, 1eaa, 2nzt, 2h88, 3j9u. TCA cycle, and Pyruvate kinase where from http://pdb101.rcsb.org/ and used with permission.

inner membrane, which is finally utilized in the rotating [25] ATPase complex V to generate ATP.

In situations of energy abundance, glucose is metabolized in non-oxidative (and thus reversible) pathways, and is also polymerized to glycogen. Glycogen is synthesized through the action of glycogen synthase (GS), which in turn is inhibited through phosphorylation by glycogen synthase kinase (GSK) under regulation of Akt.

1.2 REACTIVE OXYGEN SPECIES

1.2.1 Reactive oxygen species generation and deactivation

Aerobic exercise profoundly increases oxidative metabolism, which has the potential to damage macromolecules by generating reactive free radical (e.g. $OH^{\cdot}$, O_2^{-}, & $NO^{\cdot}$) [26]. Consequently, living organisms have evolved enzymes that neutralize free radicals. Reactive oxygen species are generated by NADPH oxidases, peroxisomal metabolism, cyclooxygenases, and by "leakage" of electrons from the oxidative phosphorylation cascade. The vast majority of reactive oxygen species is generated from the latter, and specifically the oxidative phosphorylation cascade complex I and III. Reactive oxygen species are inactivated by several enzymatic cascades. The most reactive oxygen species, the superoxide anion $O_2^{\cdot-}$, is converted to H_2O_2, a less reactive oxygen species by superoxide dismutase (SOD). The fate of H_2O_2 is decided by the enzyme responsible for their full inactivation: symmetrical cleavage to H_2O by catalase, thioredoxin oxidation by peroxidase, or glutathione (GSH) oxidation by glutathione peroxidase yielding GSSG and H_2O.

1.2.2 Reactive oxygen species in skeletal muscle health

Reactive oxygen species are both detrimental and necessary for metabolic health. Animal models show that interference with the enzymes involved in inactivation of reactive oxygen species lead to several complications: knocking out glutathione peroxidase-1 in mice leads to increased insulin sensitivity only after exercise [27], while glutathione peroxidase 4 knockout mice are embryonically lethal [28]. Knockout mice lacking superoxide dismutase in the mitochondria display perinatal lethality [29], while mice lacking cytosolic superoxide dismutase appear normal but have decreased survival time in an hyperoxic environment [30].

There is an unfounded perception in the general public that antioxidant supplementation is beneficial to health. In reality, several studies show that antioxidant treatments appear to have either detrimental, or no effects on human health. Notably, two independent large scale double blind placebo studies investigating the effects of β-carotene supplementation in smokers found increased risk of lung cancer and mortality [31, 32]. The effects of antioxidant supplementation in skeletal muscle glucose uptake are again contradictory: 4 weeks of vitamin E and C supplementation has been shown to blunt training-induced increases in insulin sensitivity and expression of genes responsive to exercise [33]. Conversely, 12 weeks of vitamin E and C supplementation has been shown to be without effect on training-induced improvements on glucose infusion rate [26]. While there is evidence of increased oxidative stress in individuals with insulin resistance [34], a meta-analysis of 14 studies investigating the effects of antioxidant supplementation on fasting blood glucose or insulin levels showed no beneficial effects [35].

Hormesis is a conceptually attractive explanation for the observation that antioxidant supplementation is not beneficial while endogenous antioxidant defenses are necessary. Hormesis suggests that an organism's beneficial or deleterious response to a substance is dose

dependent. Put in another way, a small amount of reactive oxygen species might be beneficial for metabolic health through changed signaling, while a larger dose might be detrimental through increased damage. Understanding how endogenously generated reactive oxygen species affect signaling cascades, will aid in further elucidating their role both as stressors and signaling molecules.

1.3 SKELETAL MUSCLE MASS REGULATION

Skeletal muscle mass is regulated by the balance between protein anabolism and catabolism. The anabolic arm of protein regulation revolves around translational regulation, while catabolic regulation involves protein ubiquitination, and proteosomal and autophagic degradation. Protein breakdown is essential for maintaining proper skeletal muscle function. Several conditions lead to skeletal muscle atrophy including aging (termed sarcopenia), cancer-induced cachexia, and spinal cord injury. The molecular mechanisms underlying the skeletal muscle atrophy induced by these conditions are probably related, but surely not identical.

1.3.1 Signaling and effectors of muscle anabolism

While the insulin signaling pathways described in section 1.1.3 regulates mainly glucose metabolism, the IGF1/IRS1/PI3K/Akt signaling axis integrates anabolic and catabolic arms of protein homeostasis. Central to control of translation, is the mTOR complex 1 (mTORC1). mTOR was first identified as a target of the bacterial macrolide rapamycin, leading to inhibition of cell proliferation and immune-responses. mTOR association with, among others, raptor forms mTORC1, while association with Rictor forms mTORC2. mTORC1 is partly regulated by a GTPase complex composed of tuberous sclerosis factor 1 and 2 (TSC1 and TSC2). Activated TSC2-TSC1 complex regulates mTORC1 activity by regulating the small monomeric G-protein Rheb. GTP bound Rheb stimulates mTORC1 activity, and the TSC2-TSC1 complex converts bound GTP into GDP, and thus inhibits Rheb. TSC2 takes input from several different signaling axis, including AMPK and Akt. AMPK phosphorylates TSC2, stimulating its GTPase activity [36], and leading to inhibition of mTORC1 activity. Akt phosphorylates TSC2 on a seperate residue, leading to more GTP being bound to Rheb, and stimulation of mTORC1 activity [37]. mTOR is further regulated by p70 S6 kinase (p70S6K) mediated phosphorylation on Ser2448 [38]. Finally, AMPK also phosphorylates raptor, and further inhibits mTORC1 activity and protein translation [39] (summarized in figure 2).

mTORC1 phosphorylates and regulates 4E-BP1 and p70S6K. 4E-BP1 inhibits protein translation by blocking ribosomal binding to the mRNA chain. 4E-BP1 phosphorylation leads to dissociation from the mRNA chain, and decreased translational inhibition. Concurrent with 4E-BP1 phosphorylation, mTORC1 activation phosphorylates p70S6K, which in turn activates the ribosomal 6 subunit (S6), regulating ribosomal biogenesis [40]. Increased phosphorylation and protein content of p70S6K, and S6, is a useful proxy for interrogating signals increasing protein synthesis. Conversely increased phosphorylation of 4E-BP1 indicates decreased protein translation, while decreased protein content of 4E-BP1 can indicate decreased expression of translational machinery.

1.3.2 Signaling and effectors of muscle catabolism

Protein degradation is necessary not only for muscle mass reduction, but also for overall metabolic health. Protein degradation is mediated by four main pathways: autophagy, proteasomal, caspases and calpains. Inhibition of either proteasomal [41] or autophagosomal [42] degradation leads to decreased skeletal muscle growth due to dysfunction, and insulin resistance [43]. Furthermore, exercise increases proteasomal and autophagic degradation in

humans [44], further highlighting the importance of protein turnover in health. While the majority of cellular proteins are degraded by the proteasomal degradation pathway [45], autophagy is also partly involved in skeletal muscle atrophy [46].Much less is known about caspases and Ca^{2+} dependent proteolytic degradation. Both calpains and caspases are thought to be involved in the initial acto-myosin degradation step [47, 48], and work in conjunction with the autophagic and proteasomal degradation pathway.

Proteolysis by the 26S proteasome is surprisingly (due to the high energy in the peptide bond), ATP-dependent. The 26S proteasome consists of the catalytic 20S complex and the 19S ATPase-containing complex. The 20S subunit is further composed of the structural α subunits, and the catalytic β subunits. The barrel shaped 20S complex incorporates the peptide to be degraded, and nucleophilic [49] residues hydrolyze the peptide chain into smaller peptide fragments. The 26S proteasome is important for muscle atrophy as illustrated by the fact that proteasomal inhibitors attenuate denervation-induced skeletal muscle atrophy [50], and that expression of proteasomal α subunits are upregulated after spinal cord injury [51, 52].

Autophagy (from the greek *αὐτόφαγος* - self-eater) can further be subdivided into macro-, micro- or chaperone-mediated autophagy. The common denominator of these three pathways is that the proteins are degraded in the lysosome, an acidic double-membrane vesicle containing proteolytic hydrolases.

Macro-autophagy (hereafter referred to as autophagy) is a multistep cascade which is initiated by the ULK complex [53]. The cytosolic proteins to be degraded are recognized by p62 [54], which then interacts with the LC3 interaction region of the LC3 proteins [55]. Conjugation of LC3 protein with either one or two phosphatidyl-ethanolamine moieties (LC3-I and LC3-II respectively) regulate the elongation of autophagosome [56]. The autophagosome is then transported along the microtubule network to the lysosome, and fusion between the autophagosome and the lysosome gives access to lysosomal hydrolases for the proteins to be degraded. Micro-autophagy differs in that it omits the cargo delivery, and instead direct invaginations in the lysosome sequesters proteins to be broken down [57]. Chaperone mediated autophagy utilizes the heat shock cognate protein of 70kDa to deliver proteins to the lysosome [58].

Whether a protein is destined to be degraded by the autophagic cascade or the proteolytic cascade is partly defined by the post-translational modification with ubiquitin. Ubiquitin is as the name implies a phylogenetically conserved protein which has a wide range of functions including cell cycle progression, signaling and protein degradation. It is a small, 8 kDa, protein that is attached via the action of E1 ubiquitin-activating enzyme, E2 ubiquitin-conjugating enzyme and E3 ubiquitin-ligase enzymes (reviewed in [59]). Ubiquitin is conjugated to a target protein either as a monomer, or as a chain of varying length, where the molecular function of the chain is dependent on both the number of ubiquitin monomers, and the linkage of the ubiquitin monomers in the chain. Poly-ubiquitination with more than 4 Lys48 linked ubiquitin monomers usually targets proteins to the proteasomal system [60]. Poly-ubiquitination linked by Lys63 destines a protein to be degraded by both the autophagic machinery [61-63] and the proteasomal degradation machinery [64], while Lys48 poly-ubiquitination appears to be more specific to proteasomal degradation than Lys63 poly-ubiquitination [65].

Two specific E3 ligases stand out in the context of skeletal muscle atrophy: Muscle Ring finger 1 (MuRF1) and Muscle F box (MAFbx also known as atrogin-1). These proteins are essential for skeletal muscle atrophy as illustrated by the fact that MuRF1 and MAFbx deficient mice have attenuated muscle atrophy after denervation [66]. MuRF1 deficient mice are resistant to dexamethasone treatment, while MAFbx are not, indicating that different atrophic

stimuli are regulated through different transcriptions factors [67]. They are also widely implicated in human conditions, where spinal cord injury is known to regulate their protein content [68] and gene expression [69].

Skeletal muscle degradation is coordinated by both long acting transcriptional regulation, and acutely by signaling cascades. The Akt signaling axis is (once again) at the nexus of catabolic regulation. Akt activation leads to the activation of mTORC1 signaling cascade as outlined above, phosphorylation and inhibition of Ulk1, and thus attenuated formation of autophagosomes [53]. Conversely, AMPK promotes autophagy by phosphorylating Ulk1 on a separate, stimulatory residue [53, 70]. Furthermore, Akt regulates transcription of proteasomal and autophagosomal effectors, by phosphorylating the forkhead box (FOXO) family of proteins [71] (Fig. 2). Phosphorylation of FOXO transcription factors leads to association with 14-3-3 binding proteins, and nuclear exclusion (as elaborated in section 1.5.1). Thus Akt stimulation inhibits autophagy through mTORC1 activation, and by inhibiting transcription of target proteins. Intriguingly, insulin resistance *per se* induces muscle atrophy in rodent models through increased proteolysis, indicating again the close coordination of energy and mass homeostasis [72].

Skeletal muscle mass plasticity is achieved by modifying the rates of protein synthesis and degradation. Spinal cord injury is a clear example of this, where skeletal muscle mass is greatly reduced during the first year (elaborated in section 1.6). Understanding the signals and mechanisms underlying this fairly severe condition, will shed light on how aging and sedentary behavior affects skeletal muscle mass and in extension health.

Signaling cascades studied in this thesis

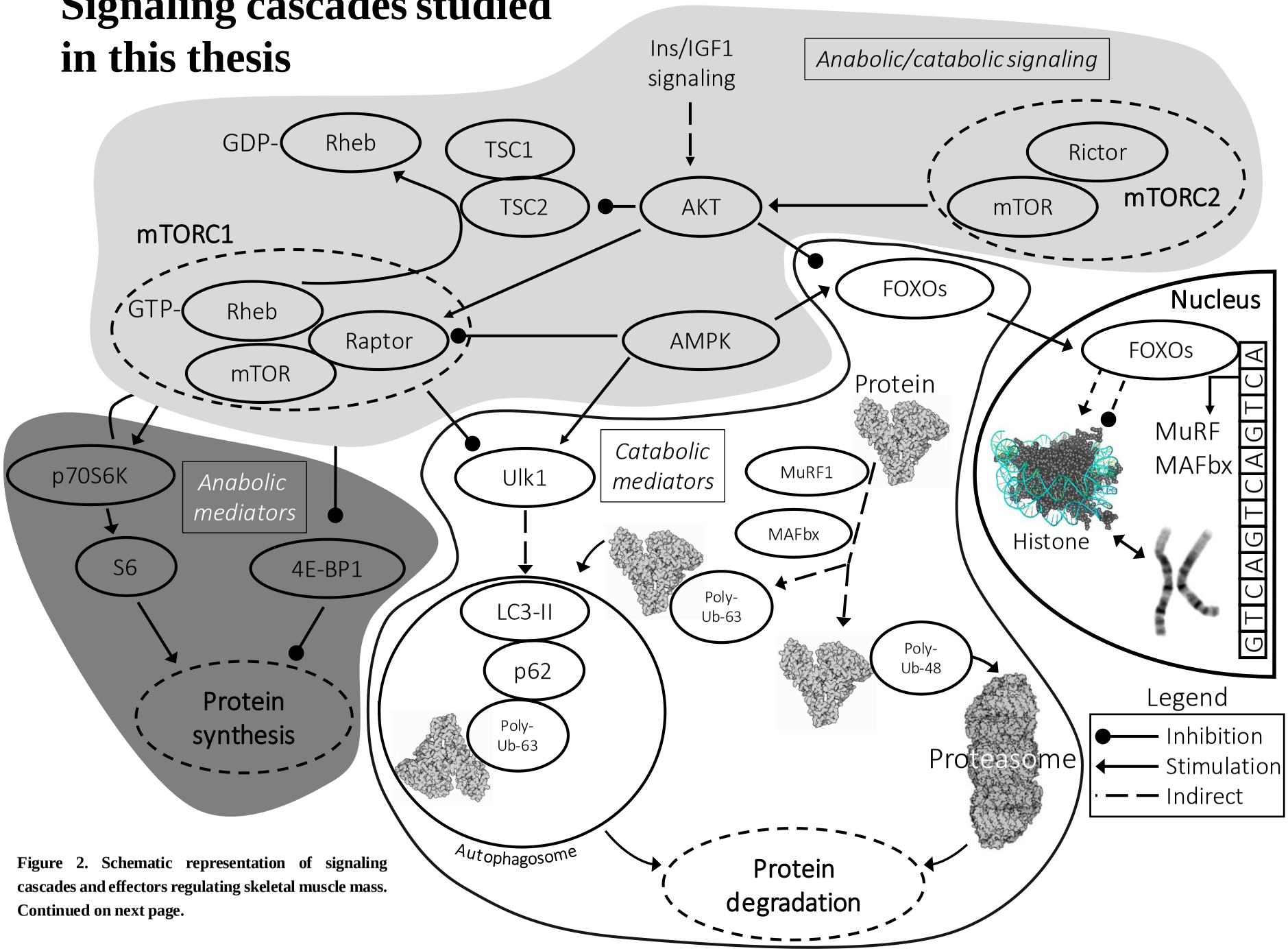

Figure 2. Schematic representation of signaling cascades and effectors regulating skeletal muscle mass. **Continued on next page.**

Figure 2. Continued from previous page. Dashed line indicates several steps not shown here, arrow indicates stimulation of activity, and oval arrow are indicates inhibition of activity. PDB files to generate figures: 1fnt, 3l5q, 1e7i and 1aoi. Chromosome image is from Wikipedia (license not necessary, public domain).

1.4 AMPK

1.4.1 AMPK structure and regulation

AMPK senses the cellular energy status and orchestrates the molecular adaptations to low energy through modulation of both signaling pathways and gene transcription. AMPK is a heterotrimeric protein comprising of the catalytic α subunit, and regulatory β and γ-subunits. The α- and β-subunits are encoded by two genes, while the γ subunit is encoded by three genes, yielding 12 potential AMPK complexes. AMPK activity is dependent on both phosphorylation and increased cytosolic AMP concentration [73]. The α-subunit contains the kinase domain mediating AMPK phosphorylation of target proteins [74]. The γ-subunit is the site of AMP detection, through 4 tandem cystathionine-β-synthase motifs, which bind and detect AMP [75]. The cystathionine-β-synthase motifs can bind both ADP and AMP, with the latter being more probable for AMPK activity *in vivo* [76]. Finally the β-subunit contains a carbohydrate binding motif that allows AMPK to interact with glycogen [77].

The mechanism and sequence of events through which AMP regulates AMPK is not completely elucidated but involves several mechanisms. Potential mechanisms of how AMP regulates AMPK include alteration of Thr172 de-phosphorylation by inhibition of AMPK phosphatases [78], allosteric regulation of AMPK [79], and AMPK phosphorylation by upstream kinases [23]. Phosphorylation of the α subunit at Thr172 is necessary for AMPK activation, and is mediated by liver kinase B (LKB1) [80] and Ca^{2+}/Calmodulin-dependent protein kinase kinase β (CaMKKβ) [81]. While LKB1 appears to be constitutively active [82], CaMKKβ activity is dependent on intracellular Ca^{2+}, thus integrating outside signals to AMPK activity. While phosphorylation is important, the allosteric regulation of AMPK by AMP is probably the major point of AMPK activity regulation *in vivo* [76].

1.4.2 AMPK and skeletal muscle mass homeostasis

As AMPK integrates information on cellular energy status, it is a critical component in regulating skeletal muscle mass and energy metabolism. The role of AMPK in the regulation of skeletal muscle is dual, increasing degradation and decreasing synthesis. As outlined above, AMPK mediated phosphorylation and inhibition of raptor leads to decreased protein synthesis through reduced mTORC1 activity. Indeed, AMPK deficient rodents have increased skeletal muscle fiber diameter and increased p70S6K phosphorylation [83], AMPK activation is concomitant with reduced 4E-BP1 phosphorylation and reduced protein synthesis during exercise [84], and AMPK activation attenuates electrical stimulation induced increase in 4E-BP1 and p70S6K phosphorylation [85]. These data suggest that AMPK activation, indicating energy deficiency, is inhibitory to protein synthesis. Conversely, AMPK activation leads to increased FOXO3 transcriptional activity, and autophagy as elaborated in section 1.5.1.

1.4.3 AMPK and energy homeostasis

AMPK activation leads to phosphorylation of substrates on motif (L/M)XRXX(S/T)XXXL [39], where X denotes any residue, and one letter amino acid abbreviations are shown. One of the most important enzymes phosphorylated by AMPK is Acetyl-CoA carboxylase (ACC), which is also the most common proxy for quantifying *in vivo* or *in vitro* AMPK activity. ACC generates malonyl CoA which in turn inhibits carnitine palmitoyl transferase 1 (CPT1) [86]. Phosphorylation of ACC by AMPK decreases the intracellular malonyl CoA concentration, lifting CPT1 inhibition and increasing influx of fatty acids into the mitochondria for β-oxidation [87].

AMPK also regulates glucose transport, storage and oxidation. Interestingly, AMPK has an insulin independent effect on GLUT4 translocation [22] (which in turn is the major glucose transporter in skeletal muscle), linking energy status to energy availability independently of hormonal signaling. AMPK stimulates GLUT4 translocation by phosphorylating and inhibiting TBC1D4, which in turn inhibits GLUT4 translocation [88]. Since AMPK is responsible for detecting cellular energy state, and is involved in the skeletal muscle mass regulation, understanding AMPK signaling modulation in atrophic conditions is key for elucidating how skeletal muscle mass is related to energy metabolism.

1.5 FOXO

In general terms, FOXO proteins are potent gene transcription regulators, which control cell cycle progression, DNA repair, antioxidant enzyme expression, autophagy and apoptosis. FOXO proteins are under the regulation of IGF1/IRS1/Akt signaling axis, which has been implicated in murine longevity models. Furthermore, both the Ames and Snell dwarf strains (with impaired growth hormone - IGF1 signaling) [89], as well as heterozygotic IGF1 knockouts [90], have increased life-span. Genetic variants of FOXO1, FOXO3 and Akt are linked to increased human life span in genome wide association studies (reviewed in [91]). This proposes a relationship between energy metabolism and longevity, and might implicate Akt signaling cascade and FOXO signaling in metabolic health.

1.5.1 FOXO protein structure and regulation

The mammalian FOXO protein family consists of 4 paralogs: FOXO1 (also denoted FKHR), FOXO3 (also denoted FOXO3a or FKHRL1), FOXO4 (also denoted AFX) and FOXO6. FOXO2 was initially thought to be an additional paralog, but is considered today homologous to FOXO3, while FOXO5 is only expressed in zebrafish [92]. FOXO proteins share an approximately 100 residue, helix turn helix, forkhead box motif mediating DNA interaction (Fig. 3). With the exception of this forkhead box motif, the FOXO proteins are disordered, and the disordered region regulates

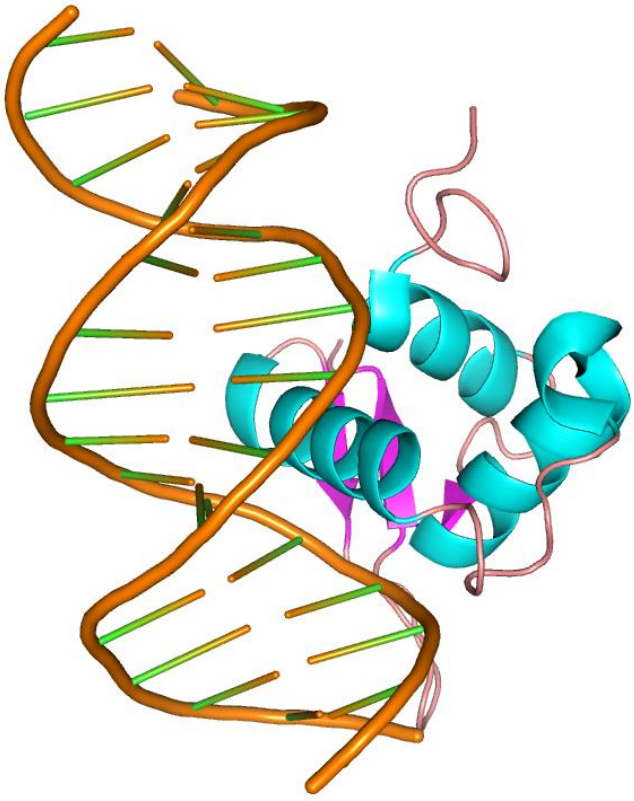

Figure 3. Crystal structure of binding domain of FOXO1 protein bound to DNA helix. PDB id 3CO7.

subcellular localization, and transcriptional activity by recruitment of additional regulatory proteins, and has several regulatory post translational modification sites for phosphorylation, acetylation and ubiquitination.

Akt mediated phosphorylation of FOXO proteins on three conserved sites leads to FOXO sequestration to the cytoplasm through interactions with the chaperone protein 14-3-3 [93, 94]. FOXO3 protein is also phosphorylated and activated by AMPK [95], while FOXO1 phosphorylation by AMPK leads to increased degradation through a different mechanism than FOXO3 [96]. Conversely, dephosphorylation of FOXO proteins by protein phosphatase 2A leads to FOXO activation [94, 97].

FOXO proteins regulate gene transcription by several mechanisms. The transactivation domain of FOXO1 interacts directly with PGC-1α to regulate gene transcription [98], and FOXO3 proteins form complexes with histone deacetylase 2 [99] repressing gene transcription, and interacts with CBP/p300 histone acetyltransferases [100] stimulating gene transcription.

1.5.2 FOXO and energy homeostasis

FOXO1 and FOXO3 are intimately involved in the regulation of energy metabolism. In liver, FOXO1 and FOXO3 regulate mitochondrial energy utilization, glycolysis and lipogenesis [101, 102]. In muscle, FOXO1 drives the expression of PDK4 [103], leading to inhibition of glucose oxidation, and also regulates the expression of lipoprotein lipase [104] and the fatty acid transporter CD36 [105] increasing the lipid oxidation. This is further supported by the observation that muscle from insulin resistant humans shows decreased expression of FOXO-target genes [106], while also showing impaired fatty acid oxidation. Thus FOXO proteins are involved in the regulation both glucose and lipid metabolism.

1.5.3 FOXO and skeletal muscle mass

FOXO proteins are involved in skeletal muscle atrophy [71]. Simultaneous ablation of FOXO1, FOXO3 and FOXO4 in mice reduces skeletal muscle loss after denervation, attenuated expression of autophagic and proteasomal gene expression, as well as attenuated increase of Lys48 and Lys63 poly-ubiquitinated proteins after fasting [107]. At the same time, the increased autophagic and proteasomal loss of skeletal muscle mass induced by the simultaneous deletion of insulin and IGF-1 receptor, is attenuated by the concomitant deletion of FOXO1-4 [108]. This highlights the important role of the Akt signaling cascade, and FOXO proteins in catabolism. Consistent with these observations, atrophic stimuli in human skeletal muscle induces increased FOXO1 protein content and expression [109].

1.5.4 FOXO and inflammation

The role of FOXO proteins in inflammatory signaling is not well understood, but is thought to involve both pro-inflammatory, and anti-inflammatory functions. FOXO1 regulates T cell infiltration by regulating expression of among other the chemokine receptor CCR7 in both T cells [110] and B cells [111]. *In vivo*, both FOXO1[110] and FOXO3 [112] deficiency leads to increased inflammation, and T cell activation. Whether this translates to regulation of muscle inflammation is currently unknown. Interestingly, corticosteroids induce loss of skeletal muscle mass, decreased inflammation, and increased FOXO expression [113], suggesting that FOXO proteins could be involved in integrating these mechanisms.

1.6 SPINAL CORD INJURY

The incidence of spinal cord injury in Sweden is between 12 and 18 cases per million and year [114]. Spinal cord injury causes partial or total interruption of neural signaling below the level of injury depending on whether the spinal cord is completely or partially damaged. The height at which the spinal cord is injured impacts whether only the legs (paraplegia) or both arms and legs are affected (tetraplegia). The lack of neural input, and subsequent skeletal muscle inactivity leads to dramatic changes in body composition, skeletal muscle fiber type, and metabolic health.

Immediately after spinal cord injury, skeletal muscle below the injury site undergoes major and rapid changes. Skeletal muscle cross sectional area is reported to decrease between 50% and 80% in the first year after spinal cord injury [115, 116]. The loss in skeletal muscle cross sectional area is accompanied by an increase in intramuscular fat [117, 118], further impairing both recovery potential, and whole-body metabolic health. Additionally, the fiber type composition of skeletal muscle switches from its normally mixed composition, to a predominantly glycolytic composition, with the majority of the fibers becoming type IIx [68, 119, 120]. The mechanism communicating and mediating the loss of skeletal muscle mass, and the changed fiber type composition is not completely understood, but involves to some extent insulin signaling, calpains, and autophagic degradation [121], with the majority of proteolysis being mediated by proteasomal degradation [122].

Spinal cord injury induces profound loss of muscle mass, which when combined with the role of skeletal muscle in glucose metabolism, leads to reduced peripheral glucose disposal during an euglycemic hyperinsulinemic clamp [13] and oral glucose challenge [118]. Isolated skeletal muscle from spinal cord injured subjects has similar levels of GLUT4 in crude membrane extracts as un-injured controls, in addition to unchanged *ex vivo* glucose uptake upon insulin stimulation [13], which combined with the observed fiber type switch is even harder to reconcile. At the same time, spinal cord injury induces changes in FOXO signaling [68] and energy metabolism enzymes [109], indicating that the observed whole-body metabolic derangements are a combination of decreased muscle mass, and changed energy handling.

2 AIMS

Skeletal muscle plays a role in metabolic health by influencing several interconnected mechanisms. As skeletal muscle (and really all) metabolic processes are imperfect, some of the potential energy can "leak" from the tightly regulated biological cascades becoming mainly reactive oxygen species. Effective handling of these reactive oxygen species is essential for proper skeletal muscle function, and in extension whole-body health. Furthermore, skeletal muscle is remarkably plastic in terms of both muscle mass, and energy metabolism according to energy availability and needs. This adaptation is mediated by AMPK, which functions as detector of the ADP to ATP ratio, and phosphorylates various targets regulating energy production and consumption, as well as other essential singling cascades in the organism. Another essential aspect of skeletal muscle health is the coordination of appropriate gene transcription depending on energy, and overall anabolic or catabolic status. FOXO is responsible for integrating the energy status and homeostatic needs through control of gene transcription. Finally, signals from FOXO, AMKP, and various other sources integrate to regulate total skeletal muscle mass. The mechanisms mediating skeletal muscle mass adaptations to changed homeostatic needs are incompletely understood. Understanding how skeletal muscle degradation is regulated will enable therapies for ameliorating the negative consequences of aging, diabetes and spinal cord injury.

In this thesis, I present four interrelated articles that center on understanding the above processes and aim to dissect the regulation of skeletal muscle plasticity and energy metabolism. Specifically, the following aims will be addressed:

1. The role of ROS on insulin action and protein signaling,
2. The role of AMPK in skeletal muscle fiber type after spinal cord injury,
3. The mechanisms regulating skeletal muscle mass after spinal cord injury,
4. The role of FOXO proteins in energy metabolism.

3 EXPERIMENTAL PROCEDURES

3.1 HUMANS STUDIES

3.1.1 General clinical characteristics

Please see table 1 for volunteers participating in Study I, table 2 for spinal cord subjects participating in an 8 week training program in study II, and table 3 for spinal cord injured subjects and able-bodied controls for studies II and III. All studies were approved by the respective regional ethics committees of Victoria University, Helse Sør-Øst Trust, and Karolinska Institutet. The study protocol adhered to the principles expressed in the Declaration of Helsinki, and all subjects provided written, informed consent.

Table 1. Volunteer characteristics in study I.

Age (yr)	22.1 (3.2)
BMI (kg/m^2)	24.8 (3.0)
Height (m)	1.8 (0.1)
Weight (kg)	81.1 (14.1)
Gender (male/female)	7/1
VO2 peak (ml/kg/min)	50.6 (4)

Data are mean and SD.

Table 2. Spinal cord injured subject characteristics undergoing 8 week exercise training in study II.

Subject	Age (yr)	Height (m)	Weight (kg)	BMI	Time since injury	Injury level
A	44	1.87	87.5	25	23	C7
B	32	1.86	69	19.9	11	C6
C	38	1.85	80	23.4	7	C5
D	28	1.86	64	18.5	6	C

Table 3. Clinical characteristics of spinal cord injured subjects (SCI) and able-bodied controls (AB) in studies II and III, data are mean and sem.

Study	2		2 & 3			2			3	
	AB (compared to chronic SCI)	Chronic SCI (compared to AB)	Complete SCI			Incomplete SCI			AB (compared to 12 months of SCI)	12 months SCI
Months after injury	NA	>12	1	3	12	1	3	12	NA	12
Age, yr	33 (2)	44 (3)	33 (4)			49 (5)			48.7 (2.3)	43.3 (5.8)
BMI, kg/m2	25 (1)	26 (2)	24 (1)	24 (0.4)	25 (0.8)	24 (0.4)	25 (0.4)	25 (0.4)	25.9 (0.9)	24.3 (1.0)
ASIA Motor score	NA	26 (4)	19 (4)	21 (5)	24 (5)	40 (12)	72 (6)	81 (2)	N.A.	
Injury level										
C4		0	0	0	0	0	0	0		1
C5		1	6			5				0
C6		4	1			1				1
C7		1	0	0	0		0	0		0
Th3		0	0	0	0	0	0	0		2
Th5		0	0	0	0	0	0	0		1
Th8		0	0	0	0	0	0	0		1
Th12		0	0	0	0	0	0	0		1

Data are presented as means and standard error of mean.

3.2 NAC STUDY

3.2.1 Cycle ergometer

Participants performed a 55 minute bout of cycling exercise at a workload corresponding to 65% of their $\dot{V}O_{2peak.}$ Following this, the workload was increased to that which corresponded to 85% of their VO_{2peak} for the final five minutes to maximize the physiological demands of the exercise session.

3.2.2 Euglycemic hyperinsulenimic clamp

Insulin sensitivity was determined using a hyperinsulinemic-euglycemic. Briefly, 3 hrs after the exercise bout, insulin (Actrapid; Novo Nordisk, Bagsvaerd, Denmark) was infused (initial bolus 9 $mU.kg^{-1}$ then continuously at 40 $mU/m^2.min$) for approximately 120 min, with plasma glucose maintained at approximately 5 $mmol.L^{-1}$, using variable infusion rates of 25% v/v glucose. Blood glucose concentration was assessed every 5 min using a glucose analyzer (YSI 2300 STAT Plus™ Glucose & Lactate Analyser, Australia). Glucose infusion rates (GIRs) were calculated during steady state, defined as the last 30 min of the insulin-stimulated period and expressed as glucose (milligrams) per body surface area (square meter) per minute. Insulin sensitivity was expressed via the M value, where mean glucose infusion rate (I, in mg/kg/min) over the final 30 min of the insulin clamp is divided by the mean insulin concentration in mU/L (M/I: glucose infusion rate/insulin concentration).

3.2.3 NAC infusion

N-acetylcysteine (NAC; Parvolex, Faulding Pharmaceuticals, Melbourne, Australia) was infused intravenously with an initial loading dose of 62.5 $mg.kg^{-1}.hr^{-1}$ for the first 15 min, followed by a constant infusion of 25 $mg.kg^{-1}.h^{-1}$ for the next 80 minutes using a syringe pump (Graseby 3400, Graseby Medical, UK). Plasma NAC concentration was later analyzed by reversed-phase ultra high performance liquid chromatography.

3.3 SPINAL CORD INJURY STUDY

3.3.1 Spinal cord injury subjects

The spinal cord injured individuals received standard upper body physical therapy, and postural stability exercises during the time studied.

3.3.2 Spinal cord injury electrically stimulated ergometry

The training period consisted of seven exercise sessions per week, with one session per day for 3 days and two sessions per day for 2 days. The training bouts were carried out on a computer-controlled electrical stimulation exercise ergometer (ERGYS-I-Clinical Rehabilitation System; Therapeutic Alliances, Fairborn, OH). All electrically stimulated leg cycling sessions were supervised by a physician and a physiotherapist. No electrically stimulated leg cycling bouts were performed during the 48 h before muscle biopsies were obtained.

3.4 MUSCLE BIOPSY PROCEDURES

The volunteers participating in study I were provided with a food parcel the day before the experiment (14 MJ, 80% carbohydrate) and instructed to abstain from alcohol, exercise

and caffeine to standardize pre-experimental muscle glycogen content. Any diet inconsistencies occurring prior to the first trial were replicated for the second trial. Muscle samples were obtained from the middle third of the *vastus lateralis* muscle using the percutaneous needle biopsy technique. After injection of a local anesthetic into the skin and fascia (1% Xylocaine, Astra Zeneca, Australia), a small incision was made and a muscle sample taken (approximately 100-200 mg) using a Bergström biopsy needle with suction. Each biopsy was taken from a separate incision, 1-2 cm distal from the previous biopsy. Muscle samples were washed free of blood and dissected of any other tissue then immediately frozen in liquid nitrogen. The volunteers of study II, and study III used a similar biopsy technique while in a postprandial state.

3.5 ANIMAL STUDIES

3.5.1 Animal housing conditions

Animal experiments were approved by the Regional Animal Ethical Committee (Stockholm, Sweden). Male C57BL/6J mice (30 week old) were purchased from Janvier (France). Mice received *ad libitum* access to water and standard rodent chow (Lantmännen, Sweden), and were housed on a 12 h light/dark cycle.

3.5.2 Plasmid design

FOXO1dn negative sequence was the same as previously described [123] consisting of amino acids 1-256. FOXO3dn was designed by aligning murine amino acid sequence to previously described dominant negative human sequence [124] yielding a 1-249 amino acid sequence. The FOXO1dn and FOXO3dn amino acid sequences obtained were optimized and converted to nucleotide sequences by GeneArt, and plasmids including empty control vector were synthesized by GeneArt (Invitrogen GeneArt, ThermoFisher Scientific, Rockford, IL).

3.5.3 Plasmid electroporation

Following one week of acclimatization, *tibialis anterior* muscle was transfected with either a control plasmid or plasmid encoding for FOXO1dn or FOXO3dn (Invitrogen GeneArt, ThermoFisher Scientific, Rockford, IL). Mice were anesthetized with isoflurane before hyaluronidase (30 µl of 1 unit/µl) transdermal injection of the *tibialis anterior* muscle. Mice were allowed to rest in individual cages for 2 h, after which they were again anesthetized with isoflurane. Plasmids (30 µg) were injected in the *tibialis anterior* muscle of each leg transdermally, and constructs were electroporated with 220 V/cm in 8 pulses of 20 milliseconds using an ECM 830 electroporator (BTX Harvard Apparatus, Holliston, MA).

3.5.4 Modified oral glucose tolerance test

One week post-electroporation, mice were fasted for 4 h, and glucose uptake was measured *in vivo* using a modified oral glucose tolerance test. A bolus of glucose (3 gm/kg) was administered through oral gavage, and [^{3}H] 2 deoxy-glucose (4.5 µl of 2-[^{3}H]deoxy-D-glucose/100 µl of saline/animal, 1 mCi/ml) was injected intraperitoneally. Mice were terminally anesthetized using avertin 120 min after the glucose gavage, and the *tibialis anterior* muscle was dissected, washed clean in phosphate buffered saline, and rapidly frozen in liquid nitrogen for subsequent determination of [^{3}H]glucose uptake. Frozen muscle samples were homogenized in ice-cold buffer (10% glycerol, 5 mM sodium pyrosulfate, 13.7 mM NaCl, 2.7 mM KCl, 1 mM $MgCl_2$, 20 mM Tris (pH 7.8), 1% Triton X-100, 10 mM NaF, 1 mM EDTA, 0.2 mM phenylmethylsulfonyl fluoride, 1 µg/ml aprotinin, 1 µg/ml leupeptin,

0.5 mM sodium vanadate, 1 mM benzamidine, and 1 μM microcystin) with dry ice cooled mortar and pestle. Homogenates were rotated end-over-end for 1 h at 4 °C and then subjected to centrifugation at 12,000 × *g* for 10 min at 4 °C. The supernatant (30 μl) was analyzed by liquid scintillation counting. A portion of the remaining supernatant was stored at −80 °C for immunoblot analysis.

3.5.5 Cell culture growth

C2C12 myoblasts were purchased from Sigma Aldrich and propagated in high glucose DMEM supplemented with 10% fetal bovine serum and 1% penicillin–streptomycin. They were passaged every 2 days.

3.5.6 Cell culture transfection

Cells were seeded in a 6 well plate at 20 000 cells/well, and transfected with FOXO1dn, FOXO3dn, or control, using Lipofectamine 3000 according to manufacturer instructions. Experiments were performed 48 h after transfection.

3.6 ANALYTICAL METHODS

3.6.1 Immunoblot analysis

Portions (30 – 60 mg) of the muscle samples were freeze-dried and dissected free of visible fat, blood, and connective tissue at room temperature. The specimens were homogenized in 0.6 ml of ice cold lysis buffer (137 mM NaCl, 1 mM $MgCl_2$, 2.7 mM KCl, 1 mM EDTA, 20 mM Tris, pH 7.8, 5 mM Na pyrophosphate, 10 mM NaF, 1% Triton X-100, 10% (vol/vol) glycerol, 0.2 mM phenylmethylsulfonyl fluoride (PMSF), 0.5 mM Na_3VO_4 and 1X protease inhibitor cocktail Set 1 (Calbiochem, EMD Biosciences, San Diego, CA)) or protease inhibitors (Roche Diagnostics GmbH, Mannheim, Germany). Insoluble material was removed by centrifugation at 12,000 *g* for 10 min at 4°C, and supernatant protein concentration was determined using a commercially available assay (Pierce BCA protein assay kit; Thermo Scientific, Rockford, IL). Equal amounts of protein were diluted in Laemmli buffer, separated by SDS-PAGE electrophoresis (Criterion XT Precast gel; Bio-Rad, Hercules, CA), and were transferred to PVDF membranes. Equal loading was confirmed by Ponceau S staining. The membranes were blocked with 5% nonfat dry milk in TBST (20 mM Tris, 137 mM NaCl, 0.02% Tween 20, pH 7.6) for 1 h at room temperature and incubated overnight at 4°C with appropriate primary antibodies diluted 1:1000 in TBS with 0.1% BSA and 15 mM NaN_3. Membranes were washed in TBST and incubated with the respective secondary antibodies diluted in 5% nonfat dry milk in TBST, as recommended by the supplier (Amersham, Arlington, IL). Proteins were visualized by enhanced chemiluminescence (Amersham) and quantified by densitometry using Quantitity One software (Bio-Rad).

3.6.2 Protein carbonylation

Protein carbonylation analysis was performed on snap frozen muscle samples using the OxyBlot Protein Oxidation Detection kit (Millipore, Billerica MA) as per manufacturer instructions, except lysis was performed without the addition of β-mercaptoethanol. Protein carbonylation was then determined via electrophoresis and immunoblotting as per Western blot analysis.

3.6.3 Antibodies used:

Target	Catalogue number	Company
4E-BP1	9644	Cell signaling
4E-BP1	9452	Cell signaling
Akt	9272	Cell signaling
AMPKα1	07−350	Millipore
AMPKα2	07−363	Millipore
AMPKβ1	1604−1	Epitomics
AMPKβ2 H-75	sc20146	Santa Cruz
AMPKγ1	1592−1	Epitomics
AMPKγ3	HPA004909	Sigma-Aldrich
FOXO1	12161	Abcam
FOXO3	ab47409	Abcam
GLUT4	07-1404	Millipore
GS	3839	Cell signaling
GSK3b	9315	Cell signaling
Hexokinase 2	not applicable	kind gift from Oluf Pedersen
LC3A/B	L8918	Sigma-Aldrich

MAFbx	sc-166806	Santa Cruz
MHC I, IIa, and IIx	not applicable	kind gift from Stefano Schiaffino
MitoProfile Total OXPHOS Human	ab110411	Abcam
mTOR	2983	Cell signaling
MuRF1	sc-32920	Santa Cruz
MitoProfile total OXPHOS Rodent	ab110413	Abcam
p-4EBP1 Thr37/46	2855	Cell signaling
p62	P0067	Sigma-Aldrich
p70S6K	9205	Cell signaling
p-ACC Ser79	3661	Cell Signaling
p-Akt Ser473	9271	Cell signaling
p-Akt Thr308	4056	Cell signaling
p-AMPKα Thr172	2531	Cell Signaling
p-FOXO1 Ser256	9461	Cell signaling
p-FoxO3 Ser253	13129	Cell signaling
p-GS Ser641	3891	Cell signaling
p-GSK3b Ser9	9323	Cell signaling
p-mTOR Ser2448	5536	Cell signaling

p-mTOR Ser2448	600-401-422	Rockland
p-p70S6K Thr389, Thr421/Ser424	2708	Cell signaling
Proteasome 20S α	ab22674	Abcam
p-S6 Ser235/236	2211	Cell signaling
p-STAT1 Tyr701	9171	Cell signaling
raptor	2280	Cell signaling
S6	2317	Cell signaling
STAT1	9172	Cell signaling
TSC2	4308	Cell signaling
Ubiquitin linkage-specific Lys48	ab140601	Abcam
Ubiquitin linkage-specific Lys63	ab179434	Abcam

Appropriate anti-rabbit, and anti-mouse antibodies were purchased from BioRad.

3.6.4 Skeletal muscle glycogen determination

Glycogen content assay was performed on freeze dried or thawed muscle samples (from previous storage in -80^{o}C), using a commercially available kit following manufacturer instructions (Abcam). Glycogen content was normalized to dry muscle sample weight.

3.6.5 Glucose uptake in C2C12

Cells were serum starved for 4h in 1 g/L DMEM, and subsequently incubated in the absence or presence of 120 nM insulin (Actrapid Novo Nordisk, Denmark) for 30 minutes. Thereafter, myoblasts were incubated in glucose-free medium containing 2-[1,2-^{3}H]deoxy-D-glucose (1 mCi/ml; Moravek) 15 min in the absence or presence of insulin. Cells were lyzed in 0.03% SDS and analyzed for [^{3}H] content using liquid scintillation counting (WinSpectral 1414, Wallac). Each experiment was performed in duplicate, and the data is the average of five experiments.

3.6.6 GSH:GSSG measurement

Total (tGSH) and oxidized (GSSG) muscle glutathione content was determined spectrophotometrically using a commercially available kit (Bioxytech GSH/GSSG-412, Oxis Health Products, Portland, OR, USA) according to manufacturer instructions. Freeze dried muscle was dissected free of connective tissue, divided into two aliquots then powdered and weighed. Muscle was then homogensized with 80 μL.mg^{-1} (dry weight) ice-cold 5% metaphosphoric acid with and without 1-methyl-2-vinyl-pyridinium trifluoromethane sulphonate (M2VP; 10% v/v). Homogenate was centrifuged at 23 000 *g* for 15 min at 4 ºC. The resulting supernatant was diluted 1:25 (tGSH), and 1:20 (GSSG) in assay buffer. Samples, standards and blanks (50 μL) were added to a 96 well plate in triplicate, followed by 50 μL of chromagen, 50 μL glutathione reductase and just prior to measurement, 50 μL NADPH. Change in absorbance (reduction of dithiobis-2-nitrobenzoic acid) was measured at 412 nm at 30 sec intervals for 4.5 min in a spectrophotometer (xMark; Bio-Rad Laboratories, Inc., Hercules, California, USA). Pellets remaining from the centrifuged homogenate were dissolved in 1 N NaOH, heated at 60 ºC with agitation then assayed for protein content (Bio-Rad). Glutathione values reported are normalized to protein content.

3.6.7 Insulin determination

Plasma insulin concentration was determined using a 96 well ELISA insulin kit (Dako, Denmark) according to the manufacturer's protocol. Briefly, duplicates of 25 µL plasma samples and standards were combined with a conjugate diluent. A conjugate concentrate mixture was then added to each well and the plate was shaken for 1 hour. Well contents were removed then washed three times using supplied wash buffer. After washing, substrate solution was added and placed in a shaker for 10 min. A stopping solution was then added before determining absorbance at 460 nm using a micro plate reader (iMark Microplate Absorbance Reader, Bio-Rad, Denmark).

3.7 GENE EXPRESSION ANALYSIS

3.7.1 qPCR

qPCR analysis was performed on total RNA from electroporated *tibialis anterior* muscle. RNA was extracted with Trizol following manufacturer's recommendations (Life Technologies). Total RNA concentration was quantified spectrophotometrically (NanoDrop ND-1000 Spectrophotometer, ThermoFisher Scientific). RNA was reverse-transcribed to cDNA using the High Capacity cDNA RT kit and gene expression was determined by real-time PCR using SYBR Green reagent (Life Technologies, ThermoFisher Scientific).

Table 5. Primer sequences

Gene	Forward Primer	Reverse primer
Foxo1	CTGCAGATCCCGTAAGACG	GGTCACCGGTGTCTAAGGAG
Foxo3	GGAAGGGAGGAGGAGGAATG	CTCGGCTCCTTCCCTTCAG
Ccl2	AGCCAACTCTCACTGAAGCC	TTCTTGGGGTCAGCACAGAC
Ccl7	CCACCATGAGGATCTCTGCC	ATAGCCTCCTCGACCCACTT
Ccl8	TTTGCCTGCTGCTCATAGCT	TGTGAAGGTTCAAGGCTGCA
Cxcl9	ACCTCAAACAGTTTGCCCCA	ACGACGACTTTGGGGTGTTT
Cd68	AAGGTCCAGGGAGGTTGTGA	ATGAATGTCCACTGTGCTGC
Cd48	CTCGGGACCTTTCCCCAAAA	ACTAGCCAAGTTGCAGTCCA
Itgax	CCAGCCAGAGGATTTCAGCAT	CTGCAGGTGTGAAGTGAACAG
Cd3g	ACTGTAGCCCAGACAAATAAAGC	TGCCCAGATTCCATGTGTTTT
Ncr1	GAGCCAGAGGATCAACACTG	ATGGCTTTGGTCTCTCCAAGG
Ly6c	ACCCTTCTCTGAGGATGGACA	GCTGGGCAGGAAGTCTCAAT
Tbp	CCTTGTACCCTTCACCAATGAC	ACAGCCAAGATTCACGGTAGA

3.7.2 Transcriptomic analysis

Microarray analysis was performed on total RNA extracted from electroporated TA muscle utilizing the EZ RNA extraction kit, and hybridized to an Affymetrix Mouse Gene 2.1 ST array (ThermoFisher Scientific) at the core facility for Bioinformatics and Expression Analysis (BEA) at Karolinska Institutet.

3.8 STATISTICAL ANALYSIS

3.8.1 Statistical analysis in study 1

Data were analyzed by two-way (treatment x time) analysis of variance with repeated measures on both factors (IBM SPSS Statistics v20). Where significant main effects were detected, post hoc analyses were conducted with Student's *t*-tests for pairwise comparisons and adjusted for multiple comparisons. Single comparisons (insulin sensitivity) were analyzed by using a paired Student's *t*-test. Statistical significance was accepted at $p<0.05$. Raw data are presented as mean ± SD for $n=7$, and change scores are reported as fold-change of the mean, or percent difference where appropriate.

3.8.2 Statistics used in study 2, and 3

Data are reported as mean and individual values. The average phosphorylation, and lipidation ratio for each subject was calculated and the mean data for the entire study cohort is presented. Statistical significance was analyzed both with mixed-models analysis, and non-parametric Friedmans test, followed by Dunns multiple comparison test for acute spinal cord injury, and non-parametric Mann–Whitney test for comparisons between spinal cord injured subjects studied 12 months after injury versus able-bodied control subjects. Correlation analysis was performed using spearman rank correlation, and heatmap was visualized in the R programing environment using the gplots package. Data in heatmap were normalized to have mean of 0 and standard deviation of ±1 per each measured protein. Statistical significance was accepted at $p \leq 0.05$.

3.8.3 Statistical analysis in study 4

Data was analyzed in R utilizing the oligo package for the robust multi-array average normalization, and annotated using the transcriptcluster package. Transcriptome data was visualized using the factoextra and ggplots2 package. Gene set enrichment analysis was performed with the GSEA software (Broad Institute, MA) using the curated Molecular Signatures Database. All statistical tests are paired student t-test. A significance threshold was defined at $p<0.05$, except for the transcriptomic analysis, where significance was defined at $p<0.01$, with at least a 40% fold change in either direction.

4 RESULTS AND DISCUSSION

4.1 EFFECTS OF ANTIOXIDANT INFUSION ON INSULIN SENSITIVITY AFTER EXERCISE.

Antioxidant treatments attenuate the beneficial effects of exercise training [33]. We sought to study the effects of acute antioxidant treatment on exercise adaptations. This was performed by studying skeletal muscle metabolic adaptations, signaling cascades, and insulin sensitivity in 7 healthy male volunteers during: exercise, recovery and insulin infusion with the concomitant infusion of either N-acetyl-cysteine (NAC) or placebo (Fig. 4).

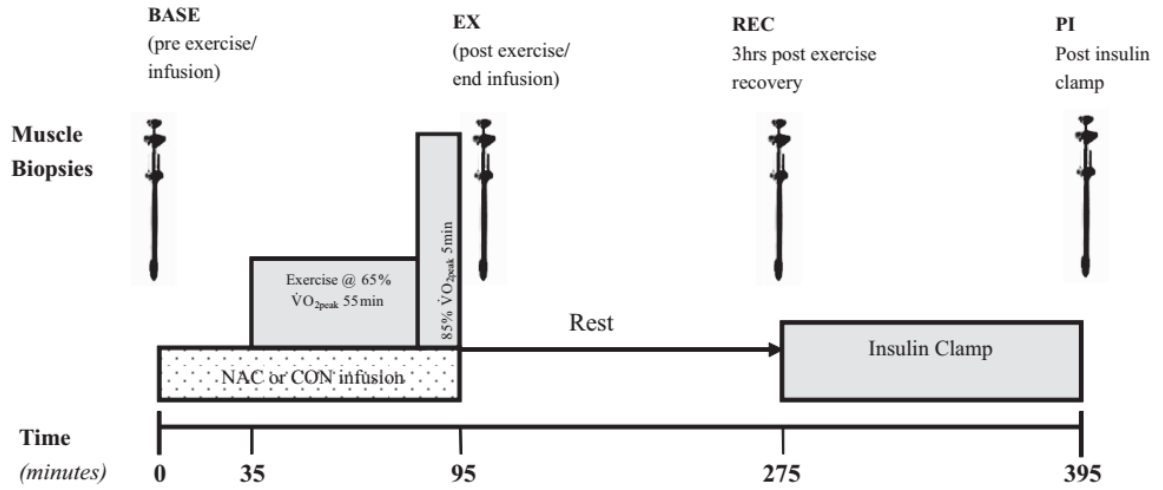

Figure 4. Schematic representation of study design. The same protocol was used in two separate occasions with either NAC or control saline infusion >7 days apart.

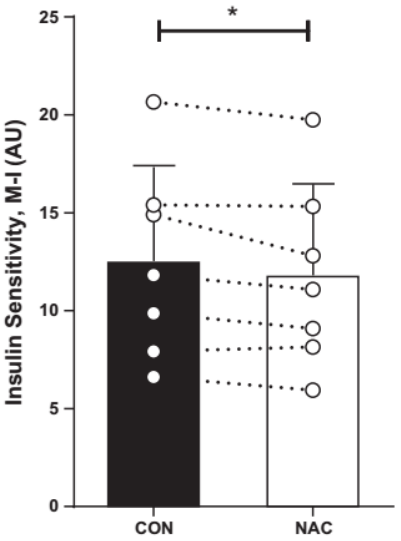

Figure 5. Insulin sensitivity compared between control or NAC infused subjects. Bars represent means, ± SD for *n*=7 , arbitrary units (AU), with individual participant responses overlayed. * = p<0.05.

NAC infusion lead to a small (~6%) but significant decrease in insulin sensitivity (Fig. 5) as defined by the M-I index (glucose infusion rate of last 30 min divided by mean insulin concentration).

Although the effect of NAC infusion on insulin sensitivity was modest, it is worth bearing in mind that the effect observed is an acute response. Furthermore, 4 weeks of treatment with antioxidant vitamins show a similar effect size on insulin infusion rate as observed here [33]. This might indicate that effects of antioxidant treatment on insulin sensitivity are rapid, and non-cumulative.

The decreased glucose infusion rate was coincident with decreased markers of reactive oxygen species activity by two different measurements methods: protein carbonylation and GSH:GSSH ratio. Protein carbonylation showed a statistical main effect for NAC infusion, and only a trend (p=0.08) for decreased protein carbonylation after exercise (Fig. 6). The GSH:GSSG ratio on the other hand had a significant main effect, as

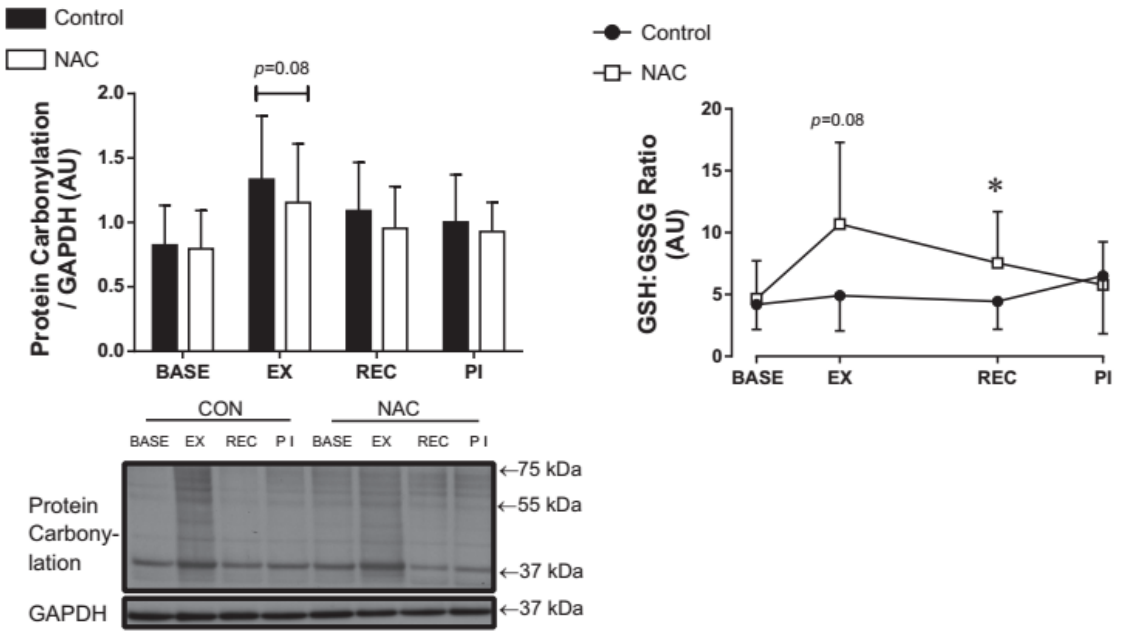

Figure 6. Effects of either NAC or saline control infusion on total protein carbonylation, and GSH:GSSG ratio. Data are means ± SD for n=7, arbitrary units (AU). * = p<0.05, p=0.08 denote trend for NAC vs. CON.

well as a trend for increased GSH:GSSG ratio immediately after exercise, and increased significantly after a 3 hour recovery period (Fig. 6).

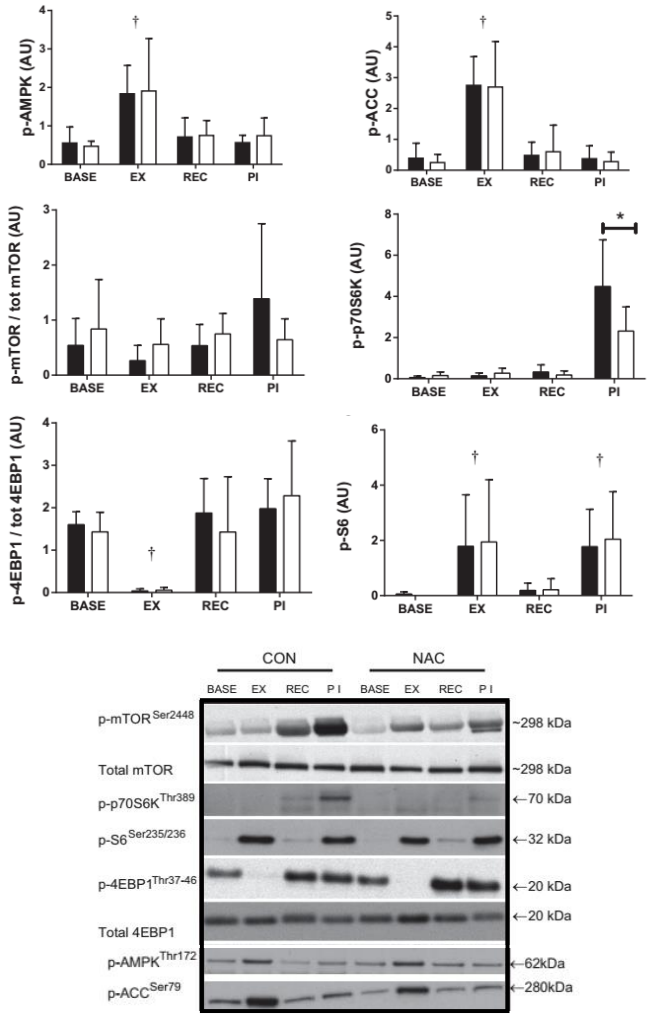

Figure 7. Effect of either NAC or saline control infusion on AMPK, and mTOR cascade protein signaling. Data are means ± SD for n=7, arbitrary units (AU). * = p<0.05 NAC vs. CON, † = p<0.05 vs BASE

While the decreased protein carbonylation was not really striking, the decreased GSH:GSSG ratio was larger. Together these data indicate that NAC infusion leads to increased antioxidant potential of endogenous systems, which translates to a small decrease in oxidized proteins.

Interestingly, the decreased insulin sensitivity was not accompanied by dramatic changes in signal transduction. Neither AMPK nor ACC phosphorylation was affected by NAC infusion (Fig. 7). This indicates that cellular energy availability was unaffected by NAC, and that AMPK is not affected directly by reactive oxygen species. Changes in the mTOR signaling cascade were contradictory. p-mTOR to total ratio, as well as p-4EBP-1 to total, and S6 phosphorylation were unaffected by NAC infusion. Conversely, p-p70S6K, the kinase responsible for S6 phosphorylation, was decreased by NAC infusion (Fig. 7), indicating that there is a dissociation of normal p70S6K function with NAC infusion, or that the phosphorylation/dephosphorylation of p70S6K is affected by other upstream molecules that are themselves responsive to oxidative stress. One fascinating interpretation of the attenuated p70S6K, could be that antioxidant supplementation blunts protein translation, and that reduced protein translation is interfering with the positive effects of exercise.

Additionally, one must consider the pharmacological effects of NAC in the context of insulin sensitivity and exercise. While NAC is considered to be a precursor for cysteine and GSG, it can also affect disulfide bridges through its thiol-disulfide exchange activity [125]. This leads to reduction and breakage of disulfide bonds, which in itself can have signaling activity. Whether the effects observed here are due to scavenging of reactive oxygen species, or by changes in the overall redox state is unknown and warrants further study.

4.2 EFFECTS OF SPINAL CORD INJURY ON SKELETAL MUSCLE COMPOSITION, METABOLISM AND SIGNALING.

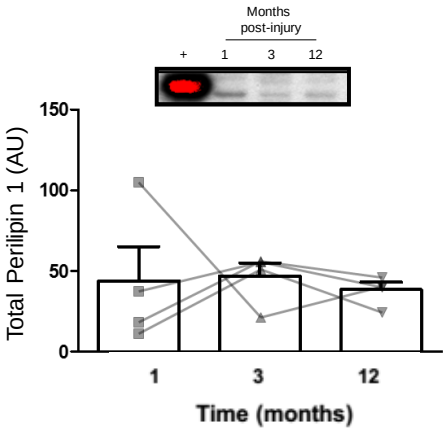

Figure 8. Protein content of lipid droplet protein perilipin 1 during the first year after spinal cord injury. Representative Western blot is shown above with positive control (mouse adipose tissue) and 1, 3 and 12 months after spinal cord injury. Red color indicates overexposure (signal saturation). Data are means ± sem, arbitrary units (AU), with individual participant responses overlayed. n=5.

Spinal cord injury leads to increased intramuscular fat [117, 118]. This opens the possibility that any observed increases in protein content or phosphorylation are due to replacement of skeletal muscle by fat. We do not detect evidence of this, as the protein content of the lipid droplet coating protein perilipin 1, is not changed during the first year after spinal cord injury (Fig. 8).

4.2.1 AMPK activation and subunit composition, oxidative phosphorylation enzymes, and MHC-proteins after spinal cord injury.

Spinal cord injury changes both composition, and energy metabolism of affected skeletal muscle. Thus we sought to quantify the AMPK subunit distribution, activity, and its correlation with mitochondrial complex protein content and fiber type distribution. These parameters were studied in able-bodied controls, individuals with complete longstanding spinal cord injury, and complete spinal cord injury during the first year after injury.

AMPK phosphorylation on Thr172, and phosphorylation of ACC on Ser79, decreased by 12 months after spinal cord injury, indicating that AMPK signaling activity is reduced during the first year after spinal cord injury (Fig. 9). This coincided with decreased protein content of AMPK subunit β1, and γ1, as well as increased protein content of AMPK subunit γ3 (Fig. 9). Conversely, incomplete spinal cord injury lead only to increased protein abundance of AMPK γ1 subunit (Fig. 7 in study II). Together these data indicate that skeletal muscle atrophy, instead of decreased neuronal signaling (due to incomplete spinal cord injury), induces a shift in energy metabolism as AMPK signaling is decreased, and changed AMPK subunit distribution.

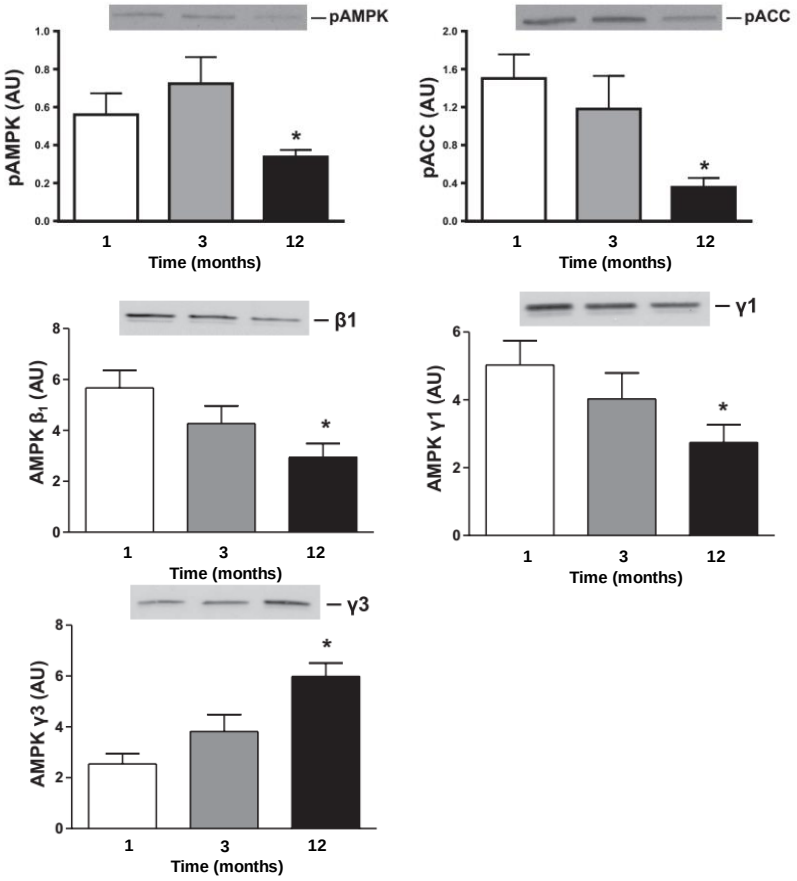

Figure 9. AMPK signaling changes and AMPK β1, γ1, and γ3, subunit composition in skeletal muscle from subjects with spinal cord injury during the first year after injury. * p < 0.05. Representative Western blots are presented above each graph. Values are presented as means ± SE, arbitrary units (AU). n = 7.

With long standing injury, we detected only decreased γ1 subunit and increased γ3 subunit protein abundance, indicating that the decrease in AMPK β1 subunit abundance observed during the first year is transient (Fig. 10). This might indicate that the β1 and α2 subunit are involved in regulating skeletal muscle mass and energy metabolism before skeletal muscle reaches steady state after chronic spinal cord injury.

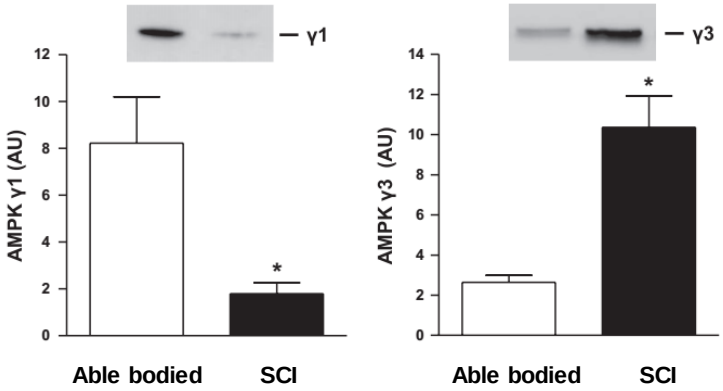

Figure 10. AMPK γ1 and γ3 subunit abundance in skeletal muscle from able-bodied individuals and subjects with long standing spinal cord injury. *p < 0.05. Representative Western blots are presented above each graph. Values are presented as means ± SE, arbitrary units (AU). n = 6–8.

The changes in AMPK signaling and isoform distribution are coincident with decreased abundance of mitochondrial complex proteins, and MHC-I protein, as well as increased MHC-IIa protein abundance after 12 months of complete spinal cord injury (Fig. 11). This suggests that changes in AMPK could be involved in the changes in MHC-distribution, and mitochondrial oxidative phosphorylation cascade.

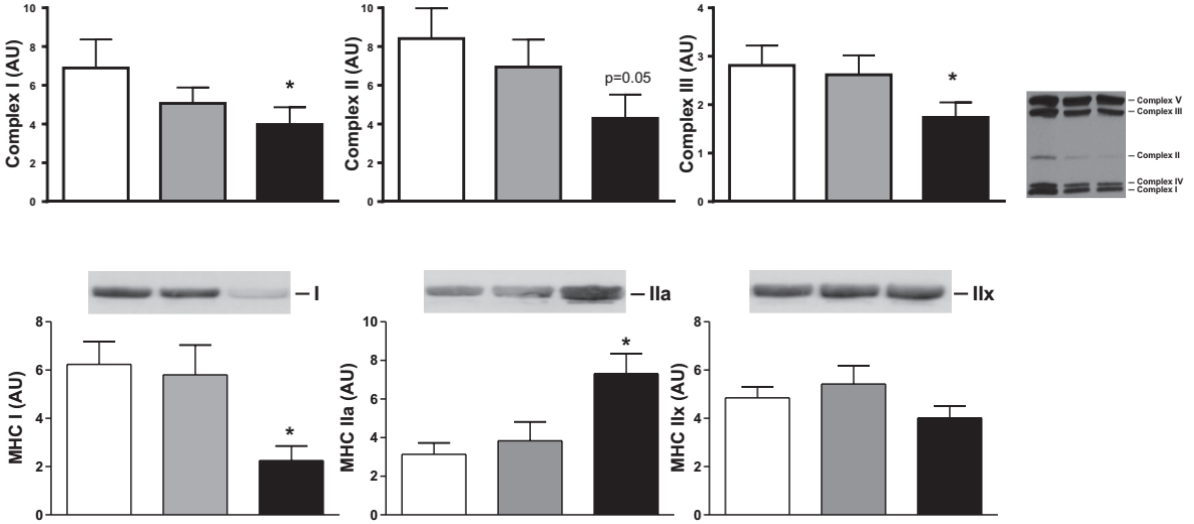

Figure 11. Protein content of mitochondrial complex proteins and MHC-protein content composition in skeletal muscle from subjects with spinal cord injury during the first year after injury. *P < 0.05. Representative Western blots are presented above each graph. Values are presented as means ± SE, arbitrary units (AU). n = 7.

Conversely, long standing spinal cord injury leads to almost complete absence of MHC-I protein, and increased protein content MHC-IIa and MHC-IIx (Fig. 12). This provides evidence to suggest that the increased protein content of MHC-IIx occurs after 12 months.

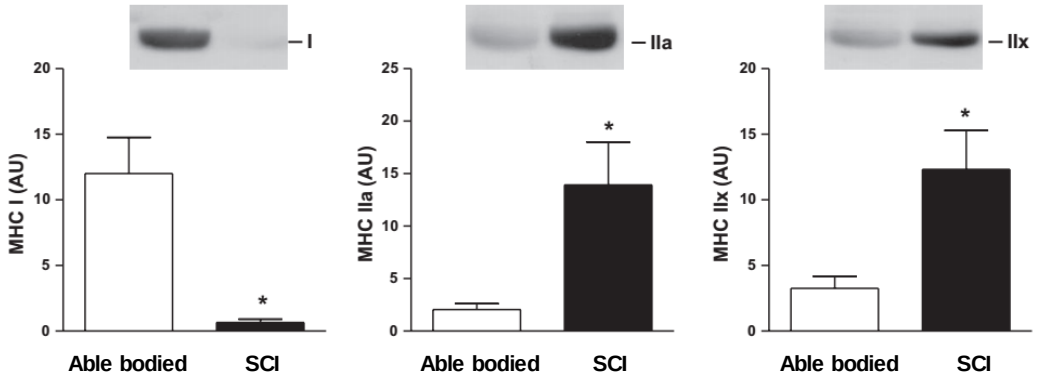

Figure 12. Protein abundance of MHC-isoforms in skeletal muscle from able-bodied individuals and subjects with long standing spinal cord injury. *p < 0.05. Representative Western blots are presented above each graph. Values are presented as means ± SE, arbitrary units (AU). n = 6–8.

The change in AMPK signaling and subunit composition could be due to either adaptive changes to the energy homeostasis of skeletal muscle, or it could be a consequence of the skeletal muscle fiber type switch [126] due to spinal cord injury. As electrically stimulated skeletal muscle training of spinal cord injured individuals shows increased AMPK protein content [127], it is plausible that the lower energy flux due to inactivity is driving the decreased AMPK signaling detected here. Measuring AMPK activity in low energy flux conditions and intact neural signaling before fiber type switch (such as unloading induced by bed rest) will

elucidate the whether changed AMPK signaling precedes the changes in skeletal muscle composition.

4.2.2 Effectors and signaling molecules regulating skeletal muscle atrophy

While it is known that spinal cord injury induces a large decrease in skeletal muscle mass, the mechanisms mediating the decrease in muscle mass are not completely understood. Decreased skeletal muscle mass can conceivably be a consequence of decreased protein synthesis, increased protein degradation, or both. Furthermore, the rate of decrease during the first year is not linear. The rate of loss is highest during the first 6 weeks, and continues at a slower rate thereafter [115]. To better understand how human skeletal muscle mass is regulated we quantified the signalling proteins regulating protein translation, proteasomal, and autophagic degradation at 1, 3 and 12 months after injury, as well as in able-bodied controls.

mTOR protein content and phosphorylation, as well as protein content of raptor, the mTORC1 defining complex was decreased during the first year after spinal cord, indicating that anabolic signalling is decreased by spinal cord injury (Fig. 13). This was accompanied by decreased protein content of the ribosomal protein S6, an indirect indicator of protein translation (Fig.14). Together, the decreased phosphorylation and protein content of mTOR, and raptor, as well as the decreased S6 protein content and phosphorylation, indicate that at least one of the components underlying the physiological observation of decreased skeletal muscle mass after spinal cord injury is decreased protein translation.

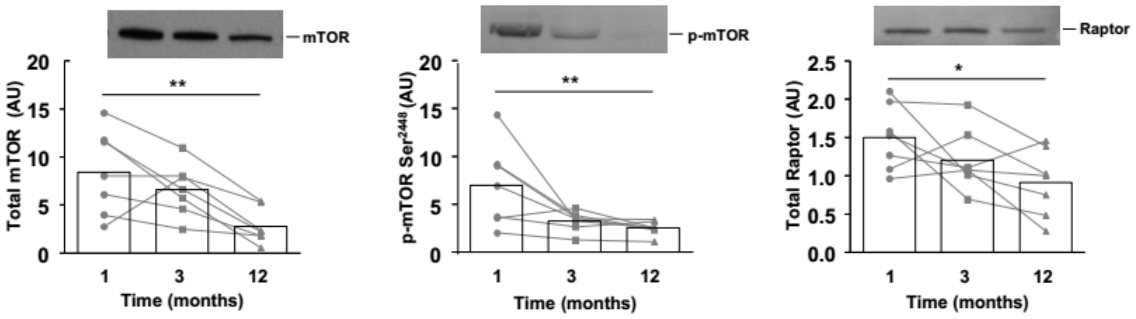

Figure 13. Changes in mTOR protein and phosphorylation, and mTORC1 complex protein raptor during the first year after spinal cord injury. Bars represent mean values, and individual data is plotted as gray line for n=7. Representative Western blots are presented above each graph. Values are arbitrary units (AU); *p<0.05 and **p<0.01.

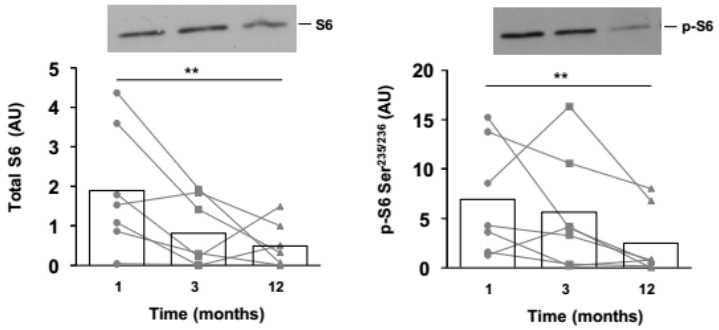

Figure 14. Protein content and phosphorylation of the ribosomal protein S6. Bars represent mean values, and individual data is plotted as gray line for n=7. Representative Western blots are presented above each graph. Values are arbitrary units (AU). **p<0.01.

Before proteins are degraded, they need to be modified by ubiquitin ligases. We found that the transcription factor FOXO3, regulating transcription of both autophagic machinery and the ubiquitin ligases MuRF1 and MAFbx [71] decreased during the first year after injury (Fig. 15). This suggests that the degradation potential of skeletal muscle is at its highest at 1 month post injury, as the decreased protein content of the ubiquitin ligases decreases after that point.

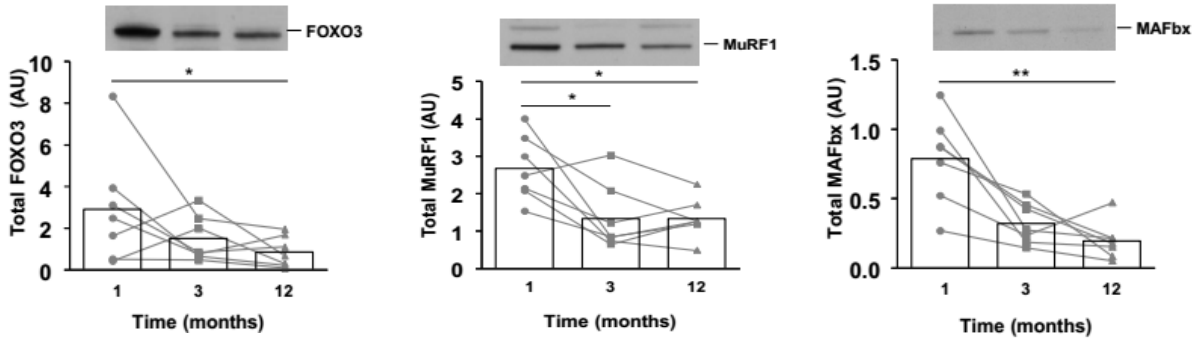

Figure 15. Protein content of FOXO3, and the skeletal muscle E3 ubiquitin ligases MuRF1 and MAFbx. Bars represent mean values, and individual data is plotted as gray line for n=7. Representative Western blots are presented above each graph. Values are arbitrary units (AU); *p<0.05 and **p<0.01.

This is interesting to contrast with rodents undergoing corticoid induced muscle atrophy, as different atrophic stimuli induce skeletal muscle atrophy through different mechanisms. MuRF1 deficient animals are protected from corticoid induced muscle atrophy, and corticoids do not increase FOXO3 protein content [67], indicating that corticoid induced skeletal muscle atrophy is under FOXO1-MuRF1 control axis. We found that the protein content of MAFbx correlates positively with both FOXO1 and FOXO3 (Fig. 16), while MuRF1 does correlate with either. Although not causative, this observation implies that in spinal cord injury, as opposed to corticoid induced muscle atrophy, MAFbx is under direct control of FOXO1 and FOXO3 while MuRF1 is not.

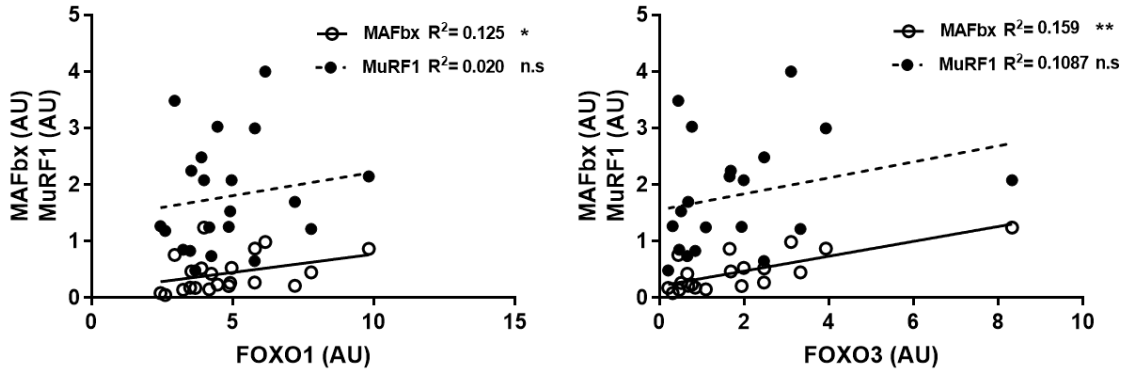

Figure 16. Correlation analysis of MAFbx (open circles) and MuRF1 (closed circles) with total FOXO1 and FOXO3 protein content. Values are arbitrary units (AU); *p<0.05 and **p<0.01. n=7.

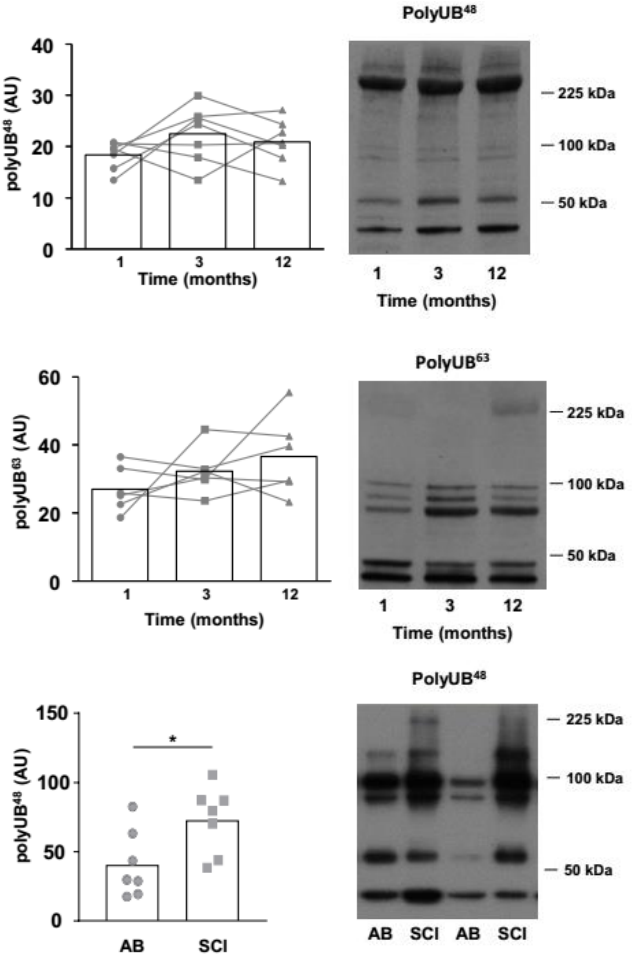

Figure 17. Poly-ubiquitination of proteins with either Lys48, or Lys63 during the first year after spinal cord injury, and comparing 12 months after injury to able-bodied controls. Bars represent mean values, and individual data is plotted as gray line for n=7 (n=6 for polyUb^{63} during first year). Representative Western blots are presented above each graph. Values are arbitrary units (AU); *p<0.05 and **p<0.01.

MuRF1 and MAFbx are directly involved in ubiquitination of proteins in skeletal muscle. Surprisingly, the decreased protein content of MuRF1 and MAFbx did not lead to decreased Lys48, or Lys63 poly-ubiquitinated proteins during the first year after spinal cord injury (Fig. 17). Furthermore, the total amount of Lys48 poly-ubiquitination did not correlate with MuRF1 or MAFbx, and Lys63 poly-ubiquitination correlated negatively with MuRF1 (Fig. 18), further highlighting the disconnection between ubiquitination and MuRF1 and MAFbx in spinal cord injured skeletal muscle atrophy.

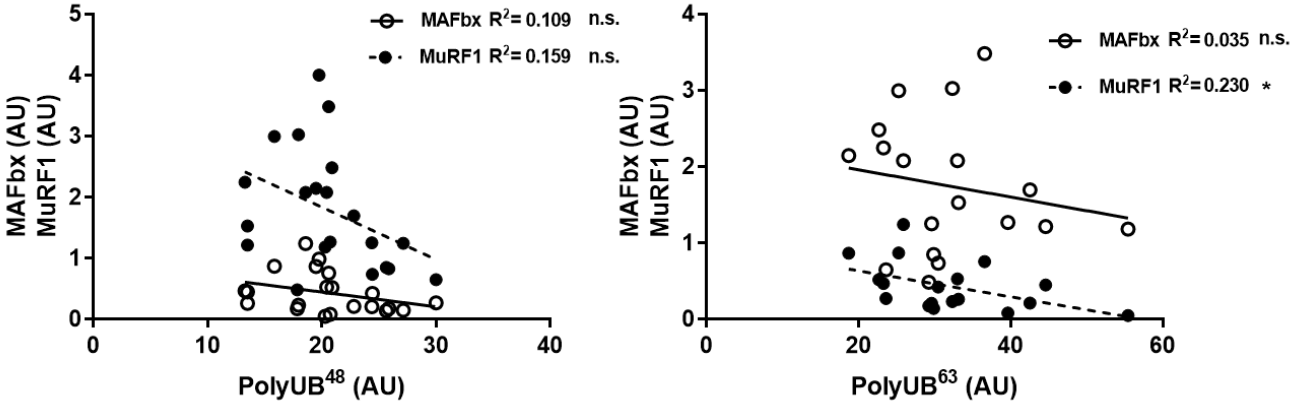

Figure 18. Correlation analysis of MAFbx (open circles) and MuRF1 (closed circles) with total poly-ubiquitination linked at Lys48 or Lys63 protein content. Values are arbitrary units (AU); *p<0.05 and n=7 for PolyUb^{48} and n=6 for PolyUb^{63}.

The observation that the decreased protein content of MuRF1, and MAFbx does not translate to attenuated ubiquitination of proteins can be explained by either decreased degradation of proteins, leading to their accumulation, or by other ubiquitin ligases acting in spinal cord injured muscle. Considering that ablation of MAFbx and MuRF1 does not lead to completely abolished denervation-induced skeletal muscle atrophy [66], both these possibilities are plausible. Moreover, there were more poly-ubiquitinated proteins with Lys48 at 12 months when compared to able-bodied controls (Fig. 17). The most plausible explanation is that there is increased protein degradation, since it is quite implausible that proteasomal degradation is lower in spinal cord injured subjects compared to able-bodied controls. The absent, or even negative correlation between MuRF1 and MAFbx and Lys48 and Lys63 poly-ubiquitin implicates again that either there is accumulation of Lys68 and Lys63 poly-ubiqutininated proteins due to decreased degradation, or that other other E3 ligases not measured play an additional role in ubiquitination after spinal cord injury.

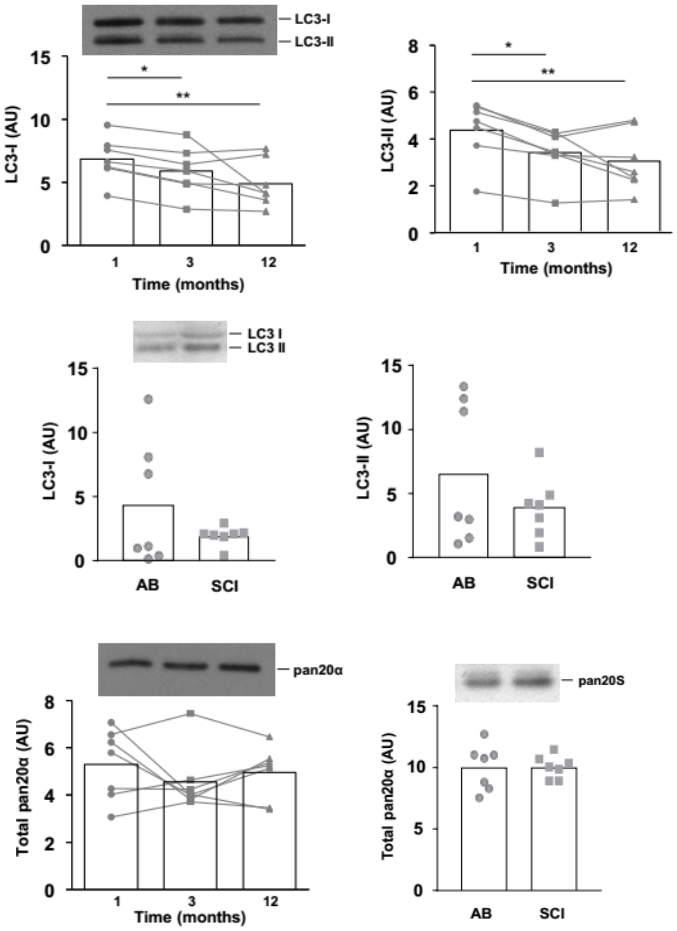

Figure 19. Protein content of autophagy and proteasomal mediating degradation during the first year after spinal cord injury and when compared to able-bodied controls. Bars represent mean values, and individual data is plotted as gray line for n=7. Representative Western blots are presented above each graph. Values are arbitrary units (AU); *p<0.05 and **p<0.01.

Breakdown of skeletal muscle proteins can be mediated by either autophagic or proteasomal degradation. We detected decreased abundance of the autophagosome initiating proteins, LC3-I and LC3-II, during the first year after spinal cord injury, but not when compared to able-bodied controls. Additionally, the structural α subunit of the proteasome 20S was unchanged during either the first year, or when comparing to able-bodied controls (Fig. 19). This provides evidence to suggest that there is increased formation of autophagosomes during at 1 month, which returns to baseline by 12 months. The unchanged Lys48 poly-

ubiquitination during the first year after spinal cord injury, together with the increased Lys48 poly-ubiquitination when comparing 12 months of spinal cord injury to able-bodied control, suggests that proteasomal degradation is increased during the first year, and remains higher than able-bodied controls.

As both mTOR and AMPK stimulate autophagy, the decreased mTOR protein content in figure 13, and decreased AMPK signaling observed in figure 9 further support the notion that autophagy is higher at 1 month after spinal cord injury. It is also possible that the transiently increased autophagosomal degradation proposed here, is mediating the decreased mitochondrial complex proteins, and the decrease in MHC-I and IIa proteins observed in figure 11.

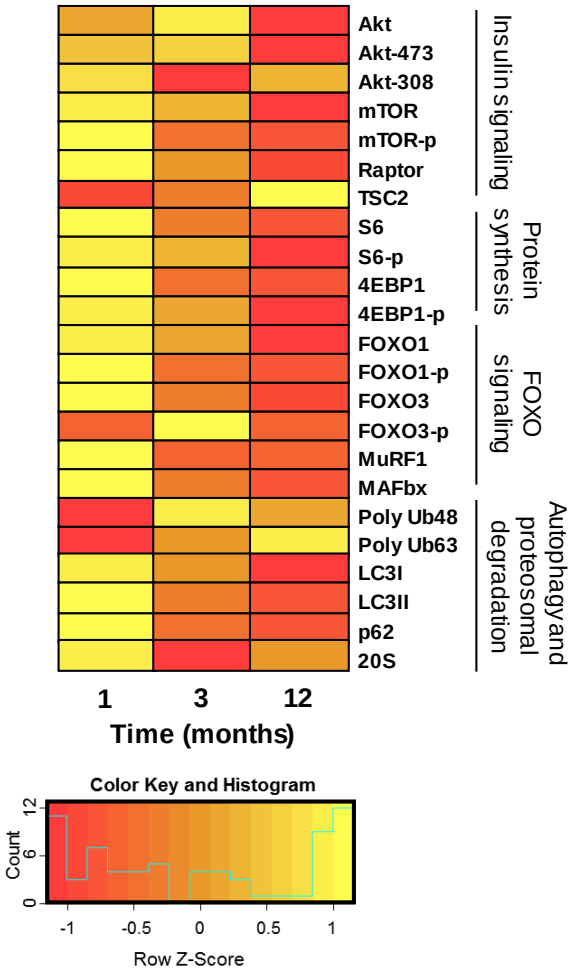

Figure 20. Heatmap of all measured proteins during the first year after spinal cord injury. Heatmap is not applicable on able-bodied controls compared to 12 months after spinal cord injury, since it is measured independently of 1, 3 and 12 months after injury. Values are z-scores, and n=7 (except PolyUb^{63} n=6)

Figure 20 shows changes during the first year of spinal of all proteins measured. Changes are normalized by scaling (mean=0, and standard deviation ± 1). One striking observation is that the protein content of most measured molecules is decreased at 3 and 12 months. This could indicate that skeletal muscle metabolic signaling is decreased, and that there is an increase in other proteins not measured here. Together, these data highlight the mechanisms underlying muscle plasticity in terms of adaptations to extreme inactivity.

4.3 THE ROLE OF FOXO PROTEINS IN SKELETAL MUSCLE METABOLISM.

Spinal cord injury leads to decreased total protein content of FOXO3, and decreased phosphorylation of FOXO1 (Fig. 3B and 3D, study III). This raises the possibility that the metabolic derangements observed in spinal cord injured individuals could partly be explained by altered transcription of metabolic genes in addition to the decreased skeletal muscle mass. To further investigate the effects of FOXO proteins on the metabolism of skeletal muscle, we electroporated *tibialis anterior* muscle with a plasmid containing either FOXO1 modified to lack its transactivation domain (FOXO1dn), similarly modified FOXO3 protein (FOXO3dn) or empty control vector (Fig. 21). The FOXOdn constructs lacking the transactivation domain bind to the DNA, and compete out endogenous FOXO or other transcription factors proximal to the binding site, leading to inhibition of gene transcription. Each animal received FOXOdn construct or control vector in the contralateral leg. Glucose uptake, insulin stimulated transcriptome profile, and signaling proteins were analyzed 7 days after transfection.

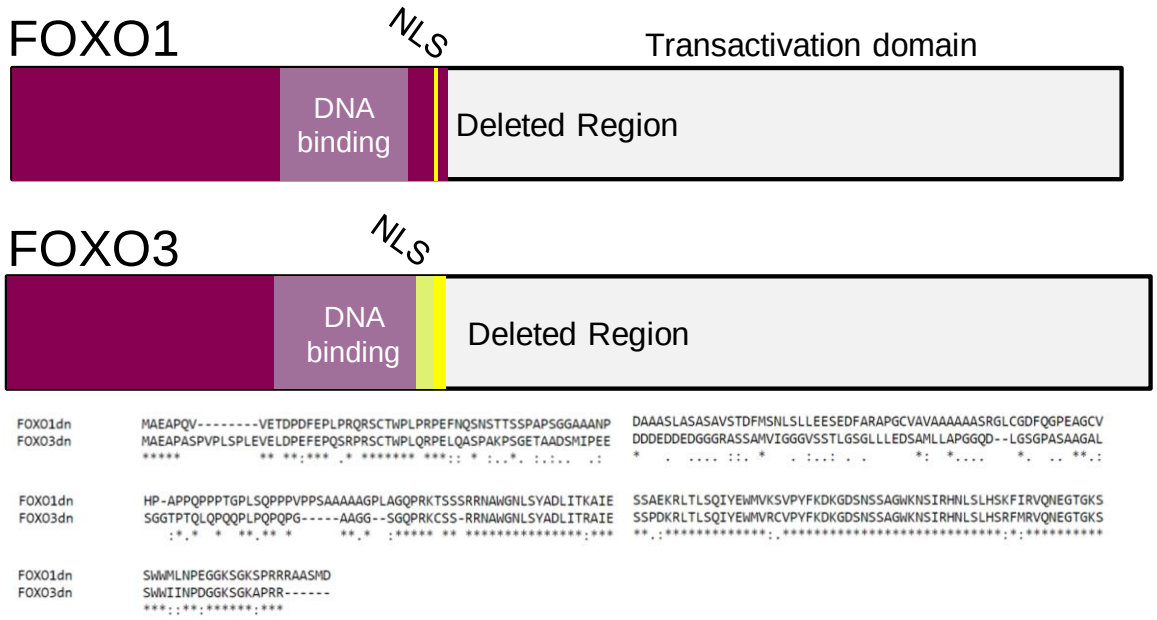

Figure 21. Schematic of FOXO1dn and FOXO3dn constructs showing, DNA binding domain, nuclear localization signal (NLS), and transactivation domain. Single amino acid alignment is shown below, with * indicating identical residues, : indicates strongly similar residues, and . weakly similar residues. Overall similarity between constructs was 58%.

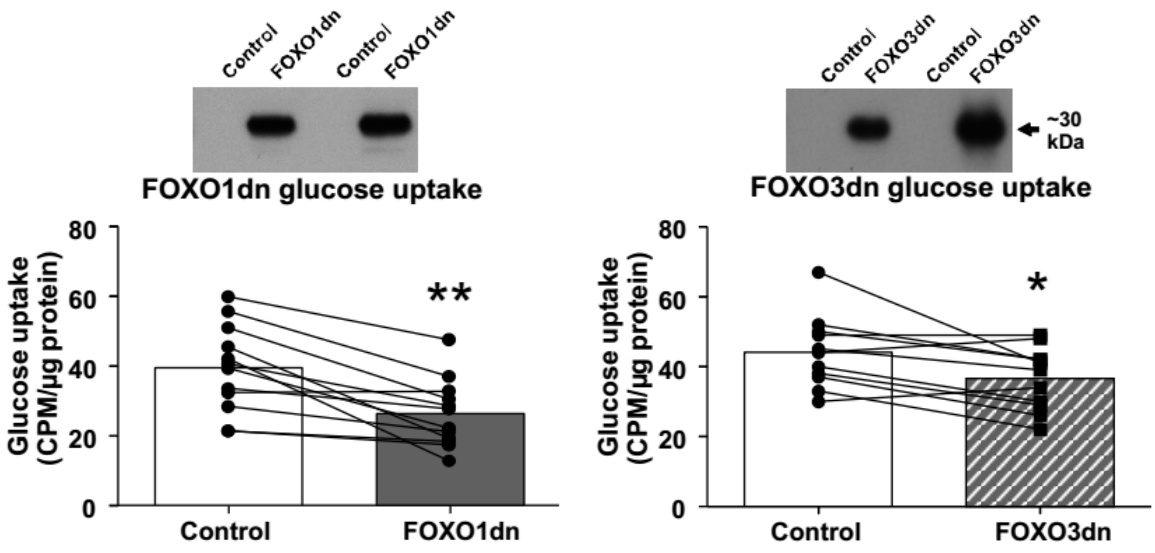

Figure 22. FOXO1dn and FOXO3dn transfection overexpression of FOXOdn protein. 2DOG uptake in *tibialis anterior* muscle in control leg and FOXOdn transfected leg. Data are mean with individual fold changes for paired muscle samples overlayed. *n*=12 mice per construct, *p<0.05, and **p<0.01.

Electroporation lead to efficient overexpression of both FOXOdn constructs, and decreased glucose uptake by 35% for FOXO1dn transfection and 20% for FOXO3dn transfection, indicating that FOXO1 and FOXO3 binding sites are involved in the regulation of glucose uptake in skeletal muscle (Fig. 22). The decrease in glucose uptake is partly explained by the decreased GLUT4 protein content (Fig. 23).

While the decrease in GLUT4 protein content after FOXO1dn transfection was larger (40%), the decrease after FOXO3dn transfection was modest (10%). This led us to investigate whether additional mechanisms could be involved in the FOXOdn induced changes in glucose uptake. Thus, we performed a transcriptomic analysis of skeletal muscle from a subset of mice.

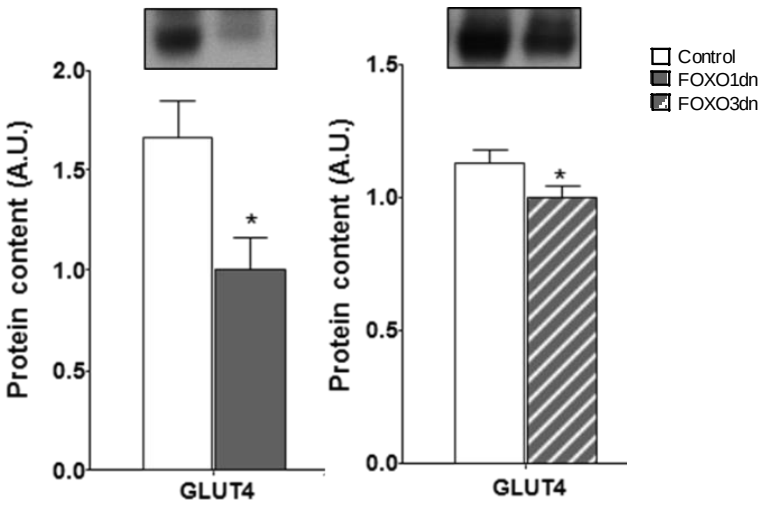

Figure 23. GLUT4 protein content in *tibialis anterior* of mice electroporated with either empty vector (open bars), FOXO1dn (gray bar), or FOXO3dn (striped bar). Data are mean ± SEM for paired muscle samples. n=12 mice per construct, *p<0.05.

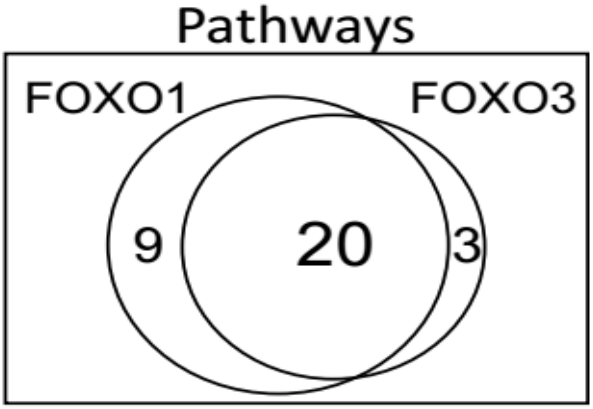

Figure 24. Overlap of gene sets enriched after FOXO1dn or FOXO3dn transfection. n=6.

Gene set enrichment analysis revealed several gene sets to be enriched by either construct. The overlap of affected gene sets between FOXO1dn and FOXO3dn was large, with 20 pathways being affected by both constructs, and 9 unique gene sets for FOXO1dn and 3 unique gene sets for FOXO3dn (Fig. 24). This indicates that FOXO1 and FOXO3 binding sites have similar physiological functions.

Among the gene sets enriched after FOXO1dn and FOXO3dn transfection were pathways involved in inflammation and oxidative phosphorylation (Fig. 25). Protein content of oxidative phosphorylation complex IV and V were downregulated by FOXO1dn transfection, while complexes II, III and IV, were downregulated by FOXO3dn transfection (Fig. 26).

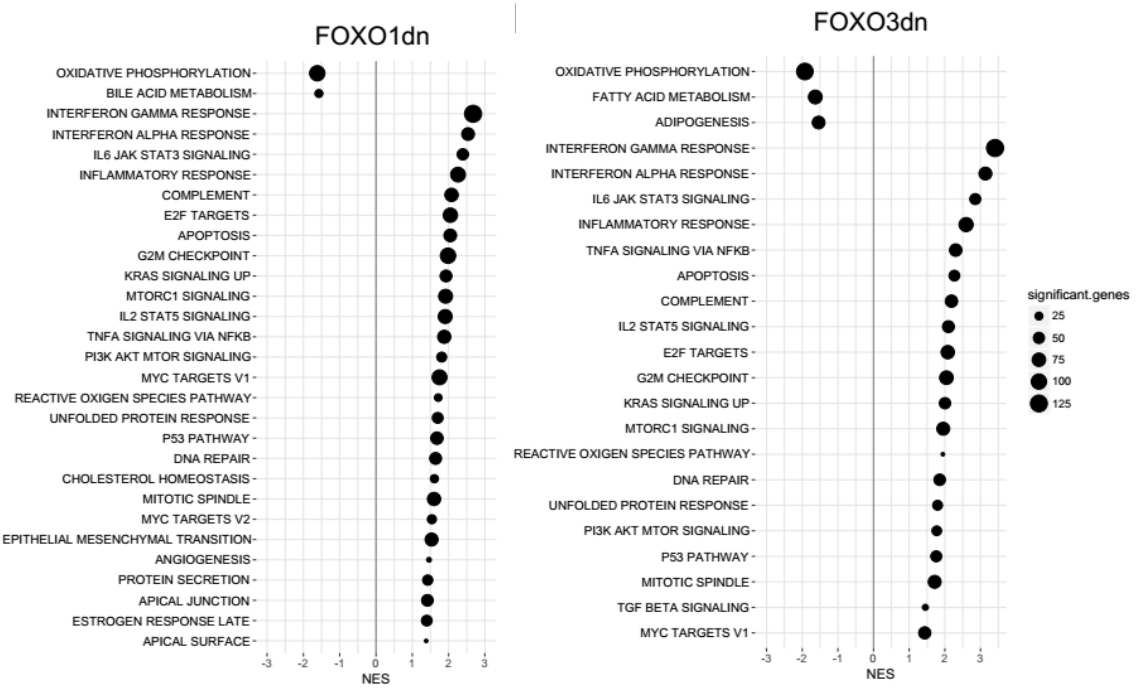

Figure 25. Gene sets enriched after FOXO1dn or FOXO3dn transfection. n=6 mice, all indicated pathways are significant at FDR<0.05.

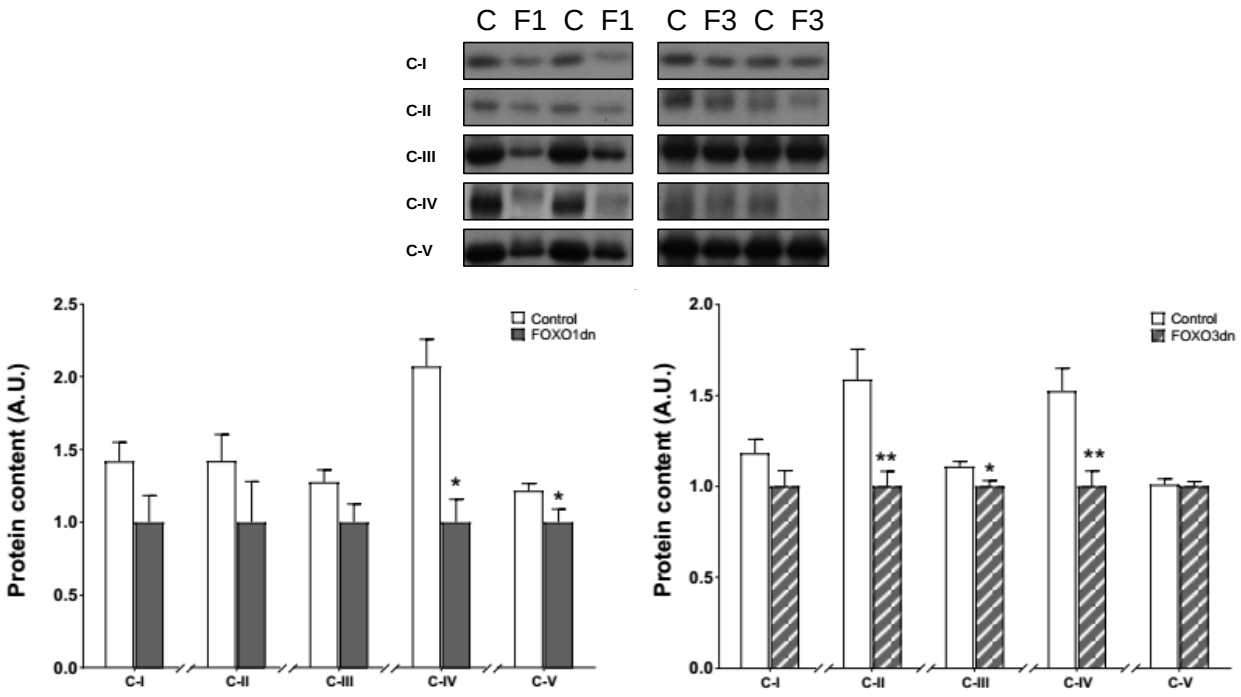

Figure 26. Protein content of complex I-V after FOXO1dn or FOXO3dn transfection. Data are mean ± SEM. *n*=11 mice, *p<0.05, and **p<0.01.

Together, these data indicate that FOXO1 and FOXO3 binding sites regulate mitochondrial gene expression in addition to GLUT4, and suggest that these two mechanisms are synergistic in affecting glucose uptake. Interestingly, genes encoding for mitochondrial protein complexes have dual origin both from the nucleus and the mitochondrial DNA. The transcription factor responsible for mitochondrial genome regulation, Tfam, was not affected by FOXOdn transfection (data not shown), indicating that either FOXO1 and FOXO3 binding sites are directly regulating nuclear genes encoding mitochondrial complex proteins, or that FOXO1 and FOXO3 binding sites affect other transcription factors involved in mitochondrial protein regulation.

The gene set enrichment analysis also indicated that inflammatory pathways are affected by FOXOdn transfection. This was validated by studying STAT1 protein content and phosphorylation, along with gene expression of chemokines and inflammatory cell markers after FOXOdn transfection. We detect a large increase in total STAT1 protein content by both FOXO1dn and FOXO3dn transfection, and increased STAT1 phosphorylation by FOXO1dn transfection. Furthermore, we detected increased expression of myokines *Ccl2, Ccl7, Ccl8* and *Cxcl9,* and increased expression of several inflammatory cells markers (Fig. 27).

The increased STAT1 protein content suggests that FOXO1 and FOXO3 binding sites are involved in regulation of anti-inflammatory signaling cascades. Furthermore, the increased expression of chemokines and inflammatory cell markers implicate increased skeletal muscle infiltration of inflammatory cells. Interestingly, we do not detect changes in glucose uptake after transfecting FOXO1dn and FOXO3dn into undifferentiated C2C12 myoblasts (Fig. 28). Although this suggests that systemic inflammation is a necessary factor for the observed effects of FOXOdn constructs, the absent expression of GLUT4 in myoblasts casts a doubt on this interpretation.

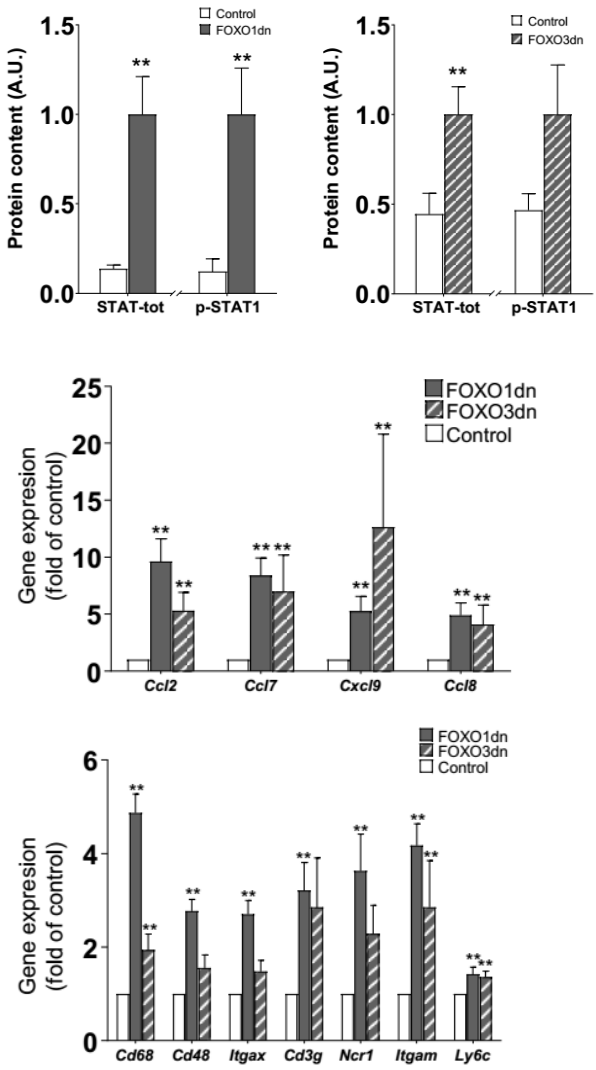

Figure 27. Protein content and phosphorylation of STAT1, and expression of chemokines, and inflammatory markers after FOXO1dn transfection (gray bars), or FOXO3dn transfection (striped bars). Data are mean ± SEM. *n*=11 mice. *p<0.05, and **p<0.01

In summary, the decrease glucose uptake, and glucose handling enzymes, as well as the increased inflammatory markers after FOXOdn transfection, indicate that FOXO1 and FOXO3 binding sites regulate skeletal muscle metabolism and inflammatory responses. Physical inactivity leads to changes in FOXO signaling, and skeletal muscle inflammation [128], raising the possibility that both are connected through the FOXO1 and FOXO3 transcription factors. Additionally, FOXO proteins regulate transcription of several antioxidant genes, suggesting that FOXO, inflammation and reactive oxygen species might together play a role in muscle homeostasis and plasticity.

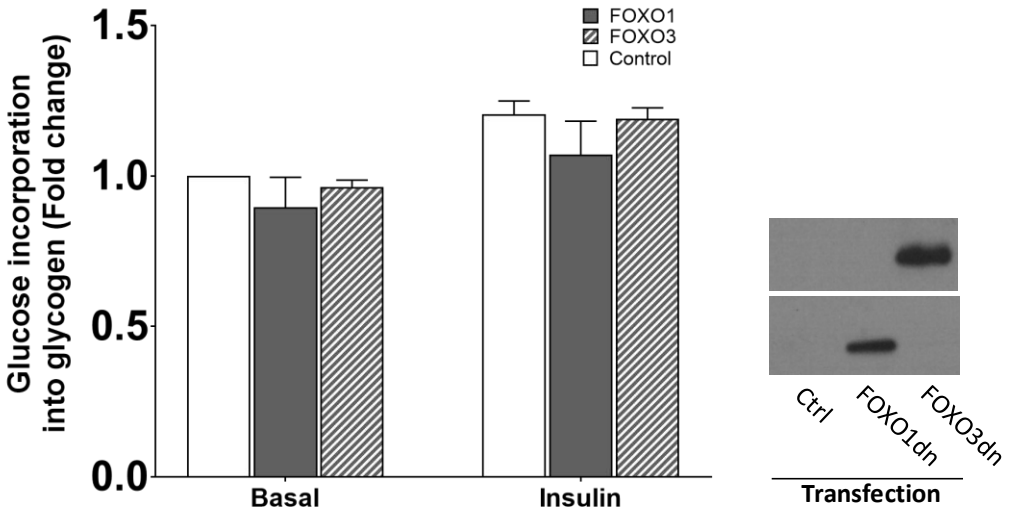

Figure 28. C2C12 myoblast basal and insulin stimulated glucose uptake after FOXO1dn (gray bars), and FOXO3dn (striped bars) transfection. Inset shows representative transfection with control, FOXO1dn or FOXO3dn plasmid. n=5 independent experiments.

5 Study limitations

There are a number of limitations with the studies presented here, some of which are inherent and some that are practical. The size of the cohorts in study I-III are rather small. We attempted to amend this by performing paired analyses where possible. In study I we utilized a crossover design where the same volunteers received both control and NAC infusion, and the spinal cord injured subjects in study II and study III donated biopsies several times over a year (with the exception of chronic spinal cord injured individuals and able-bodied controls).

Another limitation is how to measure biological processes and signaling. As biological processes are both multistep and dynamic it is challenging to establish a macroscopic phenomenon by the instantaneous measurement of a smaller part. One way to establish concerted changes in signaling (eg. Akt signaling) is to measure several downstream targets instead of the protein *per se*.

The microarray technology utilized in study IV has some technical limitation. One major limitation is determining whether a transcript is present or not. While there are methods to do this, they are prone to nucleotide sequence bias and are thus limited. We attempted to solve this problem through 2 different methods: cross validation through PCR (where all transcriptomic predicted changes were validated, data not shown), and by basing our conclusions on systems biology (mainly gene set enrichment analysis) instead of single gene measurements.

A major consideration for understanding biology is the usage of male, isogenic mouse lines. Firstly, the bigger complication is the species rather than gender. As female mice have a four day estrous cycle, experiments performed one day might be different on another due to hormonal variation (especially when studying transcription factors). One can ask how valuable these conclusions are if they cannot stand up to such variation, but since we are not intending to directly develop pharmaceuticals but rather establish phenomena this is less of an issue. Whether research performed on mice translates to humans is a more challenging question to answer. The current number of RefSeq validated genes stands at 23 911 for mice, and 18 247 in humans, and around 70% of human and mouse genes are orthologous [129], indicating that to some extent, mouse genetic biology is comparable to human. Moreover, there is great value in studying a processes in a biological context instead of in isolation as for example in a tube. Most importantly, interventions possible in mice are not even remotely ethical in human. Thus mice experiments, although limited are still of great value.

6 SUMMARY AND CONCLUSIONS

In **study I** we investigated the effects of antioxidant treatment on exercise-induced improvements on glucose handling. We found that antioxidant infusion before exercise hindered the beneficial effects of exercise on whole-body insulin signaling without affecting the canonical signaling cascades. This indicates that reactive oxygen species are involved in either signaling regulation at the level of insulin receptor, and/or on tissues other than skeletal muscle.

In **study II** we investigated the changes occurring after spinal cord injury in terms AMPK signaling, subunit composition, fiber type distribution, and energy metabolism enzymes. We found that spinal cord injury induces decreased AMPK signaling, changed subunit composition, fiber type distribution, and reduced potential for oxidative metabolism. This suggests that AMPK signaling plays a role on skeletal muscle mass regulation in humans after spinal cord injury.

In **study III** we continued our exploration of the effects of spinal cord injury on skeletal muscle health, by attempting to unravel the mechanisms underpinning decreased muscle mass. We found that proteasomal degradation is increased early in spinal cord injury, and continues to be high after 12 months, while translation and autophagy were transiently increased during the first year.

Finally in **Study IV**, we are investigated the metabolic effects of the FOXO transcription factor binding sites, a protein whose signaling is increased by spinal cord injury. We found that FOXO transcription factor binding sites regulate glucose handling, oxidative phosphorylation enzymes, and GLUT4. One additional and unexpected finding, was that FOXO proteins appeared to be involved in regulation of skeletal muscle inflammation. Together these finding are furthering our understanding of how skeletal muscle regulates glucose uptake, and how the interface between inflammation and energy metabolism is involved in health. FOXO proteins are regulated by skeletal muscle disuse, AMPK, and reactive oxygen species, potentially connecting these processes in one unified transcriptional adaptation.

Collectively, these studies are provide insight into mechanisms controlling several different aspects of skeletal muscle plasticity. This thesis work has partly resolved skeletal muscle adaptations to spinal cord injury-induced disuse, transcription factor mediated regulation of skeletal muscle glucose uptake, and the role of reactive oxygen species in skeletal muscle adaptions to exercise.

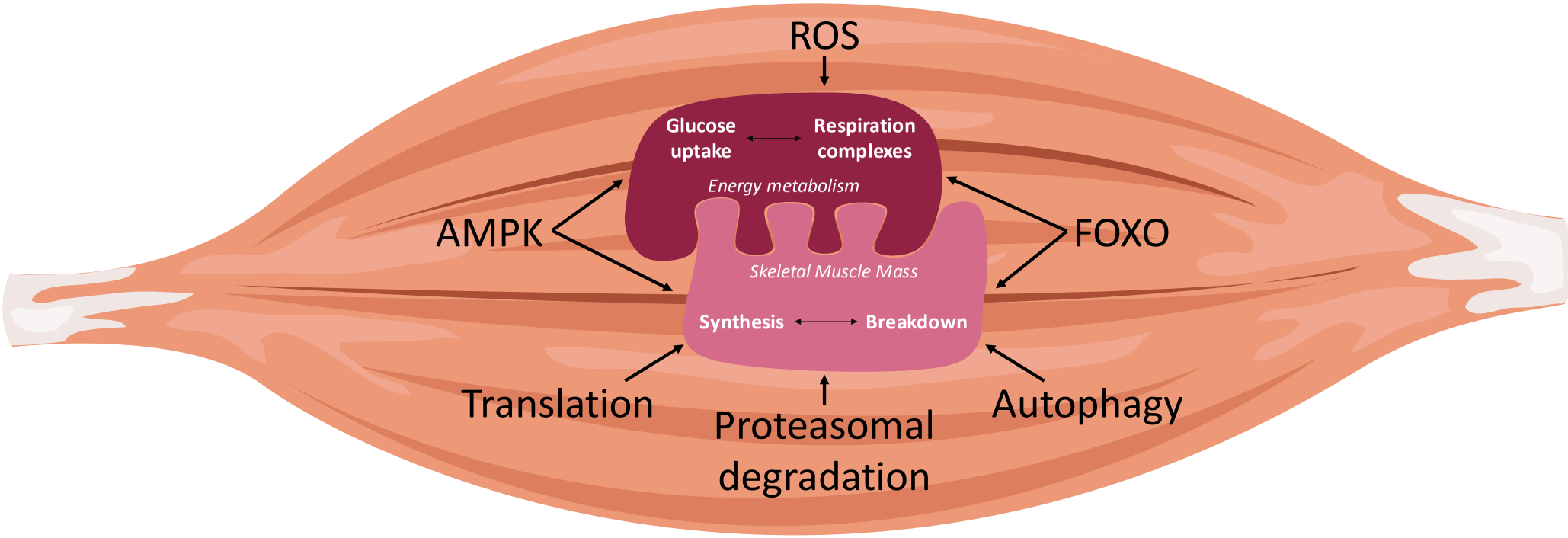

Figure 29. Schematic representation of concepts and mechanisms presented in this thesis. Muscle image is from Servier art, used with permission.

7 FUTURE PERSPECTIVE AND CLINICAL IMPLICATIONS

The future of our health looks both bright and bleak. As the human population becomes increasingly sedentary, obese, and unhealthy, the need to understand our wellbeing becomes increasingly acute. At the same time, science has never had as many participants, resources and actionable conclusions. One of these insights is that human health is a multifactorial affair, where skeletal muscle plays an important role. In this thesis I have tried to further elucidate how skeletal muscle is involved in health by studying several complementary skeletal muscle processes.

The findings in **study I**, show that reactive oxygen species are beneficial for insulin signaling. One unexplored potential of this finding is the possibility of creating therapies based on generation of reactive oxygen species instead of inhibition. Of course this would have to be finally tuned in terms of when and where in the cell they are generated. Furthermore, these findings highlight the value of preventative lifestyle interventions, as both obesity and high sugar consumption are linked to increased reactive oxygen species generation.

The findings in **study II** and **study III** are not just relevant for the fairly rare but debilitating results of spinal cord injury, but inform to some extent the effects of our how our sedentary behavior induces disuse atrophy and impaired skeletal muscle metabolism. The decreased AMPK signaling is potentially indicative of reduced ability to respond to stress and adaptations to low energy flux, while the decreased oxidative capacity is indicative of cellular damage. It is tempting to speculate on the potential beneficial effects of AMPK activation through pharmacological intervention in spinal cord injury, and in extension on sedentary behavior. **Study III** highlights targets for pharmacological interventions on skeletal muscle atrophy, by suggesting that proteasomal degradation is the most important target for intervention. Moreover, both these studies highlight the importance of early interventions after spinal cord injury.

Study I, II and III are also informative for a condition that is currently distant, but becoming tantalizingly near: wide spread human space travel. The microgravity environment of space induces both muscle atrophy through unloading, and has oxidative properties due to solar and cosmic winds [130]. Understanding the interplay of protein synthesis and degradation, with energy metabolism and reactive oxygen species will enable us to better understand the challenges of this new environment.

As both insulin resistance and skeletal muscle atrophy involve changes in FOXO signaling, **Study IV** proposes a mechanism for integrating inflammatory and energy signaling, with obesity and sedentary behavior. Since FOXO signaling plays a multitude of roles, direct modulation of FOXO signaling seems farfetched. Elucidating the gene networks controlled by FOXO transcription factors improves our understanding on how skeletal muscle metabolism is affected during disuse atrophy.

8 ACKNOLEDGEMENTS

Obviously the most read part of a thesis is the most important one.

First and foremost I extend my warmest gratitude and respect to my supervisors: Juleen, Anna, and Alex. You have taught me lessons that I will carry with me for the rest of my life. I hope.

Juleen meeting someone of your stature, skill and knowledge was slightly overwhelming the first time. I can honestly say though, that today, this has transformed into immense respect. You have taught me how to present myself, how to speak about science, and how to distill ideas into understandable communication.

Anna, your positivity has kept me going and stopped me from dwelling on negative thoughts about science and my career in more ways than I can count. You have helped me believe in my own ideas and ability, and given me perspective on when I am wrong, and when I am not.

Alex, you have given me the view of pure science, on asking questions for the sake of answering them, and discussing farfetched, crazy scientific ideas, theories and concepts.

Juleen, Anna, and Alex, together, you have taught me science, critical thinking, and guided me through a PhD. I will always remember you, and cherish my time under your guidance.

Thank you Julie, who despite our (only rarely intense) disagreements I consider a good friend. You have been the scientist at the bench who has guided, and inspired me. Rasmus, do I need to say than parta? Mladen and Petter, I will miss our very productive fikas. Melisa and Milena (or is it the other way around), thank you for filling the big office with laughter. David, I greatly appreciate all our discussions on stats, and R. Carolina, you calmness has been infectious. Thais, Nico, Brendan, Laura, Lucile and Mutsumi, you have been great company at lunch to talk about not only science but about politics, the world and everything in between. Jon, I like your humor. Arja, thank you for all the office help, and the cookies. Marie, thank you for always being more than glad to help and answer questions. Stefan, Barbro, Håkan, Ann-Marie, Tobbe, and Katrin, thank you for being a reminder that I live in Sweden, and for our interesting discussions during fika and 11 am lunches. I want to extend a whole-hearted thank you to Ulrika, PO and Emil, for the (really long) collaboration, discussions, and for the rapid and helpful feedback on our manuscript. Kasper and Ninö, you are my scientists-friends, our lunches have taught me many things. And finally, thank you Bea, you are a big reason for my pursuit of a PhD.

Thank you to the past and present members of integrative physiology: Harriet, Margareta, Megan, Lubna, Son, Max, Jonathan, Ahmed, Ana, Frederick, Laurène, Sameer, Robby, Kim, and Isabelle.

Thank you to the colleagues in the department of Physiology and Pharmacology: Vicente, Jorge, Igor, Paula, Leo, Sofia, Irené, Håkan, Johanna, Anna, Renee, and Lars.

I am grateful to the volunteers who made this thesis possible by donating a small piece of themselves.

Finally, thank you to my whole family and friends. I have not chosen my family, but I have the luck to know you. I have chosen my friends, and I am lucky to have you.

9 REFERENCES

1. Zurlo, F., et al., *Skeletal-Muscle Metabolism Is a Major Determinant of Resting Energy-Expenditure.* Journal of Clinical Investigation, 1990. **86**(5): p. 1423-1427.

2. Kelley, D., et al., *Skeletal-Muscle Glycolysis, Oxidation, and Storage of an Oral Glucose-Load.* Journal of Clinical Investigation, 1988. **81**(5): p. 1563-1571.

3. DeFronzo, R.A., et al., *The effect of insulin on the disposal of intravenous glucose. Results from indirect calorimetry and hepatic and femoral venous catheterization.* Diabetes, 1981. **30**(12): p. 1000-7.

4. Saltin, B., et al., *Fiber types and metabolic potentials of skeletal muscles in sedentary man and endurance runners.* Annals of the New York Academy of Sciences, 1977. **301**: p. 3-29.

5. Gollnick, P.D., et al., *Enzyme activity and fiber composition in skeletal muscle of untrained and trained men.* Journal of Applied Physiology, 1972. **33**(3): p. 312-9.

6. Oberbach, A., et al., *Altered fiber distribution and fiber-specific glycolytic and oxidative enzyme activity in skeletal muscle of patients with type 2 diabetes.* Diabetes Care, 2006. **29**(4): p. 895-900.

7. Lillioja, S., et al., *Skeletal muscle capillary density and fiber type are possible determinants of in vivo insulin resistance in man.* Journal of Clinical Investigation, 1987. **80**(2): p. 415-24.

8. Li, J.B. and A.L. Goldberg, *Effects of Food-Deprivation on Protein-Synthesis and Degradation in Rat Skeletal-Muscles.* American Journal of Physiology, 1976. **231**(2): p. 441-448.

9. Tiao, G., et al., *Intracellular regulation of protein degradation during sepsis is different in fast- and slow-twitch muscle.* American Journal of Physiology-Regulatory Integrative and Comparative Physiology, 1997. **272**(3): p. R849-R856.

10. Goldberg, A.L. and H.M. Goodman, *Relationship between Cortisone and Muscle Work in Determining Muscle Size.* Journal of Physiology-London, 1969. **200**(3): p. 667-&.

11. Herbison, G.J., M.M. Jaweed, and J.F. Ditunno, *Muscle atrophy in rats following denervation, casting, inflammation, and tenotomy.* Archives of Physical Medicine and Rehabilitation, 1979. **60**(9): p. 401-4.

12. Ohira, Y., et al., *Rat soleus muscle fiber responses to 14 days of spaceflight and hindlimb suspension.* Journal of Applied Physiology (1985), 1992. **73**(2 Suppl): p. 51S-57S.

13. Aksnes, A.K., et al., *Intact glucose transport in morphologically altered denervated skeletal muscle from quadriplegic patients.* American Journal of Physiology, 1996. **271**(3 Pt 1): p. E593-600.

14. Myers, M.G., Jr., et al., *IRS-1 activates phosphatidylinositol 3'-kinase by associating with src homology 2 domains of p85.* Proceedings of the National Academy of Sciences of the United States of America, 1992. **89**(21): p. 10350-4.

15. Alessi, D.R., et al., *3-Phosphoinositide-dependent protein kinase-1 (PDK1): structural and functional homology with the Drosophila DSTPK61 kinase.* Current Biology, 1997. **7**(10): p. 776-89.

16. Sano, H., et al., *Insulin-stimulated phosphorylation of a Rab GTPase-activating protein regulates GLUT4 translocation.* Journal of Biological Chemistry, 2003. **278**(17): p. 14599-602.

17. Roach, W.G., et al., *Substrate specificity and effect on GLUT4 translocation of the Rab GTPase-activating protein Tbc1d1.* Biochemical Journal, 2007. **403**(2): p. 353-8.

18. Hou, J.C. and J.E. Pessin, *Ins (endocytosis) and outs (exocytosis) of GLUT4 trafficking.* Current Opinion in Cell Biology, 2007. **19**(4): p. 466-73.

19. Richter, E.A. and M. Hargreaves, *Exercise, GLUT4, and skeletal muscle glucose uptake.* Physiological Reviews, 2013. **93**(3): p. 993-1017.

20. Wallberg-Henriksson, H. and J.O. Holloszy, *Contractile activity increases glucose uptake by muscle in severely diabetic rats.* Journal of Applied Physiology: Respiratory, Environmental and Exercise Physiology, 1984. **57**(4): p. 1045-9.

21. Wallberg-Henriksson, H., et al., *Glucose transport into rat skeletal muscle: interaction between exercise and insulin.* Journal of Applied Physiology, 1985. **65**(2): p. 909-13.

22. Hayashi, T., et al., *Evidence for 5' AMP-activated protein kinase mediation of the effect of muscle contraction on glucose transport.* Diabetes, 1998. **47**(8): p. 1369-73.

23. Hawley, S.A., et al., *5'-AMP activates the AMP-activated protein kinase cascade, and Ca2+/calmodulin activates the calmodulin-dependent protein kinase I cascade, via three independent mechanisms.* Journal of Biological Chemistry, 1995. **270**(45): p. 27186-91.

24. Niu, W., et al., *PKCepsilon regulates contraction-stimulated GLUT4 traffic in skeletal muscle cells.* Journal of Cellular Physiology, 2011. **226**(1): p. 173-80.

25. Noji, H., et al., *Direct observation of the rotation of F1-ATPase.* Nature, 1997. **386**(6622): p. 299-302.

26. Yfanti, C., et al., *Effect of antioxidant supplementation on insulin sensitivity in response to endurance exercise training.* American Journal of Physiology-Endocrinology and Metabolism, 2011. **300**(5): p. E761-E770.

27. Loh, K., et al., *Reactive oxygen species enhance insulin sensitivity.* Cell Metabolism, 2009. **10**(4): p. 260-72.

28. Yant, L.J., et al., *The selenoprotein GPX4 is essential for mouse development and protects from radiation and oxidative damage insults.* Free Radical Biology and Medicine, 2003. **34**(4): p. 496-502.

29. Lebovitz, R.M., et al., *Neurodegeneration, myocardial injury, and perinatal death in mitochondrial superoxide dismutase-deficient mice.* Proceedings of the National Academy of Sciences of the United States of America, 1996. **93**(18): p. 9782-7.

30. Carlsson, L.M., et al., *Mice lacking extracellular superoxide dismutase are more sensitive to hyperoxia.* Proceedings of the National Academy of Sciences of the United States of America, 1995. **92**(14): p. 6264-8.

31. Heinonen, O.P., et al., *Effect of Vitamin-E and Beta-Carotene on the Incidence of Lung-Cancer and Other Cancers in Male Smokers.* New England Journal of Medicine, 1994. **330**(15): p. 1029-1035.

32. Goodman, G.E., et al., *The beta-carotene and retinol efficacy trial: Incidence of lung cancer and cardiovascular disease mortality during 6-year follow-up after stopping beta-carotene and retinol supplements.* Journal of the National Cancer Institute, 2004. **96**(23): p. 1743-1750.

33. Ristow, M., et al., *Antioxidants prevent health-promoting effects of physical exercise in humans.* Proceedings of the National Academy of Sciences of the United States of America, 2009. **106**(21): p. 8665-70.

34. Tumova, E., et al., *The impact of rapid weight loss on oxidative stress markers and the expression of the metabolic syndrome in obese individuals.* Journal of Obesity, 2013. **2013**: p. 729515.

35. Akbar, S., S. Bellary, and H.R. Griffiths, *Dietary antioxidant interventions in type 2 diabetes patients: a meta-analysis.* The British Journal of Diabetes & Vascular Disease, 2011. **11**(2): p. 62-68.

36. Inoki, K., T.Q. Zhu, and K.L. Guan, *TSC2 mediates cellular energy response to control cell growth and survival.* Cell, 2003. **115**(5): p. 577-590.

37. Manning, B.D., et al., *Identification of the tuberous sclerosis complex-2 tumor suppressor gene product tuberin as a target of the phosphoinositide 3-Kinase/Akt pathway.* Molecular Cell, 2002. **10**(1): p. 151-162.

38. Chiang, G.G. and R.T. Abraham, *Phosphorylation of mammalian target of rapamycin (mTOR) at ser-2448 is mediated by p70S6 kinase.* Journal of Biological Chemistry, 2005. **280**(27): p. 25485-25490.

39. Gwinn, D.M., et al., *AMPK phosphorylation of raptor mediates a metabolic checkpoint.* Molecular Cell, 2008. **30**(2): p. 214-226.

40. Gingras, A.C., B. Raught, and N. Sonenberg, *Regulation of translation initiation by FRAP/mTOR.* Genes Dev, 2001. **15**(7): p. 807-26.

41. Kitajima, Y., et al., *Proteasome Dysfunction Induces Muscle Growth Defects And Protein Aggregation.* Medicine and Science in Sports and Exercise, 2014. **46**(5): p. 352-352.

42. Masiero, E., et al., *Autophagy Is Required to Maintain Muscle Mass.* Cell Metabolism, 2009. **10**(6): p. 507-515.

43. He, C.C., et al., *Exercise-induced BCL2-regulated autophagy is required for muscle glucose homeostasis (vol 481, pg 511, 2012).* Nature, 2013. **503**(7474): p. 146-146.

44. Jamart, C., et al., *Modulation of autophagy and ubiquitin-proteasome pathways during ultra-endurance running.* Journal of Applied Physiology, 2012. **112**(9): p. 1529-1537.

45. Rock, K.L., et al., *Inhibitors of the Proteasome Block the Degradation of Most Cell-Proteins and the Generation of Peptides Presented on Mhc Class-I Molecules.* Cell, 1994. **78**(5): p. 761-771.

46. Taillandier, D., et al., *Coordinate activation of lysosomal, Ca 2+-activated and ATP-ubiquitin-dependent proteinases in the unweighted rat soleus muscle.* Biochemical Journal, 1996. **316 (Pt 1)**: p. 65-72.

47. Du, J., et al., *Activation of caspase-3 is an initial step triggering accelerated muscle proteolysis in catabolic conditions.* Journal of Clinical Investigation, 2004. **113**(1): p. 115-123.

48. Kumamoto, T., et al., *Localization of the Ca2+-Dependent Proteinases and Their Inhibitor in Normal, Fasted, and Denervated Rat Skeletal-Muscle.* Anatomical Record, 1992. **232**(1): p. 60-77.

49. Brannigan, J.A., et al., *A Protein Catalytic Framework with an N-Terminal Nucleophile Is Capable of Self-Activation (Vol 378, Pg 416, 1995).* Nature, 1995. **378**(6557): p. 644-644.

50. Beehler, B.C., et al., *Reduction of skeletal muscle atrophy by a proteasome inhibitor in a rat model of denervation.* Experimental Biology and Medicine, 2006. **231**(3): p. 335-341.

51. Medina, R., S.S. Wing, and A.L. Goldberg, *Increase in levels of polyubiquitin and proteasome mRNA in skeletal muscle during starvation and denervation atrophy.* Biochemical Journal, 1995. **307 (Pt 3)**: p. 631-7.

52. Taillandier, D., et al., *Regulation of proteolysis during reloading of the unweighted soleus muscle.* The International Journal of Biochemistry & Cell Biology, 2003. **35**(5): p. 665-75.

53. Kim, J., et al., *AMPK and mTOR regulate autophagy through direct phosphorylation of Ulk1*. Nature Cell Biology, 2011. **13**(2): p. 132-U71.

54. Seibenhener, M.L., et al., *Sequestosome 1/p62 is a polyubiquitin chain binding protein involved in ubiquitin proteasome degradation.* Molecular and Cellular Biology, 2004. **24**(18): p. 8055-8068.

55. Pankiv, S., et al., *p62/SQSTM1 binds directly to Atg8/LC3 to facilitate degradation of ubiquitinated protein aggregates by autophagy.* Journal of Biological Chemistry, 2007. **282**(33): p. 24131-24145.

56. Kabeya, Y., et al., *LC3, GABARAP and GATE16 localize to autophagosomal membrane depending on form-II formation.* Journal of Cell Science, 2004. **117**(13): p. 2805-2812.

57. Sahu, R., et al., *Microautophagy of Cytosolic Proteins by Late Endosomes (vol 20, pg 131, 2011).* Developmental Cell, 2011. **20**(3): p. 405-406.

58. Chiang, H.L., et al., *A role for a 70-kilodalton heat shock protein in lysosomal degradation of intracellular proteins.* Science, 1989. **246**(4928): p. 382-5.

59. Lecker, S.H., A.L. Goldberg, and W.E. Mitch, *Protein degradation by the ubiquitin-proteasome pathway in normal and disease states.* Journal of the American Society of Nephrology, 2006. **17**(7): p. 1807-19.

60. Thrower, J.S., et al., *Recognition of the polyubiquitin proteolytic signal.* EMBO Journal, 2000. **19**(1): p. 94-102.

61. Wooten, M.W., et al., *Essential role of sequestosome 1/p62 in regulating accumulation of Lys63-ubiquitinated proteins.* Journal of Biological Chemistry, 2008. **283**(11): p. 6783-9.

62. Tan, J.M., et al., *Lysine 63-linked ubiquitination promotes the formation and autophagic clearance of protein inclusions associated with neurodegenerative diseases.* Human Molecular Genetics, 2008. **17**(3): p. 431-9.

63. Zemoura, K., C. Trumpler, and D. Benke, *Lys-63-linked Ubiquitination of -Aminobutyric Acid (GABA), Type B1, at Multiple Sites by the E3 Ligase Mind Bomb-*

2 Targets GABA(B) Receptors to Lysosomal Degradation. Journal of Biological Chemistry, 2016. **291**(41): p. 21682-21693.

64. Saeki, Y., et al., *Lysine 63-linked polyubiquitin chain may serve as a targeting signal for the 26S proteasome.* EMBO Journal, 2009. **28**(4): p. 359-371.

65. Jacobson, A.D., et al., *The lysine 48 and lysine 63 ubiquitin conjugates are processed differently by the 26 s proteasome.* Journal of Biological Chemistry, 2009. **284**(51): p. 35485-94.

66. Bodine, S.C., et al., *Identification of ubiquitin ligases required for skeletal muscle atrophy.* Science, 2001. **294**(5547): p. 1704-8.

67. Baehr, L.M., J.D. Furlow, and S.C. Bodine, *Muscle sparing in muscle RING finger 1 null mice: response to synthetic glucocorticoids.* Journal of Physiology, 2011. **589**(Pt 19): p. 4759-76.

68. Leger, B., et al., *ATROGIN-1, MuRF1, AND FoXO, AS WELL AS PHOSPHORYLATED GSK-3 beta AND 4E-BP1 ARE REDUCED IN SKELETAL MUSCLE OF CHRONIC SPINAL CORD-INJURED PATIENTS.* Muscle & Nerve, 2009. **40**(1): p. 69-78.

69. Urso, M.L., et al., *Alterations in mRNA expression and protein products following spinal cord injury in humans.* Journal of Physiology-London, 2007. **579**(3): p. 877-892.

70. Sanchez, A.M.J., et al., *AMPK promotes skeletal muscle autophagy through activation of forkhead FoxO3a and interaction with Ulk1*. Journal of Cellular Biochemistry, 2012. **113**(2): p. 695-710.

71. Milan, G., et al., *Regulation of autophagy and the ubiquitin-proteasome system by the FoxO transcriptional network during muscle atrophy.* Nature Communications, 2015. **6**: p. 6670.

72. Wang, X., et al., *Insulin resistance accelerates muscle protein degradation: Activation of the ubiquitin-proteasome pathway by defects in muscle cell signaling.* Endocrinology, 2006. **147**(9): p. 4160-8.

73. Frosig, C., et al., *5 '-AMP-activated protein kinase activity and protein expression are regulated by endurance training in human skeletal muscle.* American Journal of Physiology-Endocrinology and Metabolism, 2004. **286**(3): p. E411-E417.

74. Hawley, S.A., et al., *Characterization of the AMP-activated protein kinase kinase from rat liver and identification of threonine 172 as the major site at which it phosphorylates AMP-activated protein kinase.* Journal of Biological Chemistry, 1996. **271**(44): p. 27879-27887.

75. Scott, J.W., et al., *CBS domains form energy-sensing modules whose binding of adenosine ligands is disrupted by disease mutations.* Journal of Clinical Investigation, 2004. **113**(2): p. 274-284.

76. Gowans, G.J., et al., *AMP Is a True Physiological Regulator of AMP-Activated Protein Kinase by Both Allosteric Activation and Enhancing Net Phosphorylation.* Cell Metabolism, 2013. **18**(4): p. 556-566.

77. Hudson, E.R., et al., *A novel domain in AMP-activated protein kinase causes glycogen storage bodies similar to those seen in hereditary cardiac arrhythmias.* Current Biology, 2003. **13**(10): p. 861-866.

78. Davies, S.P., et al., *5'-AMP inhibits dephosphorylation, as well as promoting phosphorylation, of the AMP-activated protein kinase. Studies using bacterially expressed human protein phosphatase-2C alpha and native bovine protein phosphatase-2A(c).* FEBS Letters, 1995. **377**(3): p. 421-425.

79. Suter, M., et al., *Dissecting the role of 5 '-AMP for allosteric stimulation, activation, and deactivation of AMP-activated protein kinase.* Journal of Biological Chemistry, 2006. **281**(43): p. 32207-32216.

80. Lizcano, J.M., et al., *LKB1 is a master kinase that activates 13 kinases of the AMPK subfamily, including MARK/PAR-1.* EMBO Journal, 2004. **23**(4): p. 833-843.

81. Hawley, S.A., et al., *Calmodulin-dependent protein kinase kinase-beta is an alternative upstream kinase for AMP-activated protein kinase.* Cell Metabolism, 2005. **2**(1): p. 9-19.

82. Sakamoto, K., et al., *Activity of LKB1 and AMPK-related kinases in skeletal muscle: Effects of contraction, phenformin, and AICAR.* American Journal of Physiology-Endocrinology and Metabolism, 2004. **287**(2): p. E310-E317.

83. Lantier, L., et al., *Coordinated maintenance of muscle cell size control by AMP-activated protein kinase.* FASEB Journal, 2010. **24**(9): p. 3555-3561.

84. Dreyer, H.C., et al., *Resistance exercise increases AMPK activity and reduces 4E-BP1 phosphorylation and protein synthesis in human skeletal muscle.* Journal of Physiology-London, 2006. **576**(2): p. 613-624.

85. Thomson, D.M., C.A. Fick, and S.E. Gordon, *AMPK activation attenuates S6K1, 4E-BP1, and eEF2 signaling responses to high-frequency electrically stimulated skeletal muscle contractions.* Journal of Applied Physiology, 2008. **104**(3): p. 625-632.

86. Winder, W.W. and D.G. Hardie, *Inactivation of acetyl-CoA carboxylase and activation of AMP-activated protein kinase in muscle during exercise.* American Journal of Physiology, 1996. **270**(2 Pt 1): p. E299-304.

87. Merrill, G.F., et al., *AICA riboside increases AMP-activated protein kinase, fatty acid oxidation, and glucose uptake in rat muscle.* American Journal of Physiology, 1997. **273**(6 Pt 1): p. E1107-12.

88. Geraghty, K.M., et al., *Regulation of multisite phosphorylation and 14-3-3 binding of AS160 in response to IGF-1, EGF, PMA and AICAR.* Biochemical Journal, 2007. **407**(2): p. 231-41.

89. Bartke, A. and H. Brown-Borg, *Life extension in the dwarf mouse.* Current Topics in Developmental Biology, 2004. **63**: p. 189-225.

90. Holzenberger, M., et al., *IGF-1 receptor regulates lifespan and resistance to oxidative stress in mice.* Nature, 2003. **421**(6919): p. 182-7.

91. Kenyon, C.J., *The genetics of ageing.* Nature, 2010. **464**(7288): p. 504-12.

92. Eijkelenboom, A. and B.M. Burgering, *FOXOs: signalling integrators for homeostasis maintenance.* Nature Reviews Molecular Cell Biology, 2013. **14**(2): p. 83-97.

93. Brunet, A., et al., *14-3-3 transits to the nucleus and participates in dynamic nucleocytoplasmic transport.* Journal of Cell Biology, 2002. **156**(5): p. 817-28.

94. Singh, A., et al., *Protein Phosphatase 2A Reactivates FOXO3a through a Dynamic Interplay with 14-3-3 and AKT.* Molecular Biology of the Cell, 2010. **21**(6): p. 1140-1152.

95. Greer, E.L., et al., *The energy sensor AMP-activated protein kinase directly regulates the mammalian FOXO3 transcription factor.* Journal of Biological Chemistry, 2007. **282**(41): p. 30107-30119.

96. Barthel, A., et al., *Regulation of the forkhead transcription factor FKHR (FOXO1a) by glucose starvation and AICAR, an activator of AMP-activated protein kinase.* Endocrinology, 2002. **143**(8): p. 3183-3186.

97. Yan, L., et al., *PP2A regulates the pro-apoptotic activity of FOXO1.* Journal of Biological Chemistry, 2008. **283**(12): p. 7411-20.

98. Puigserver, P., et al., *Insulin-regulated hepatic gluconeogenesis through FOXO1-PGC-1 alpha interaction.* Nature, 2003. **423**(6939): p. 550-555.

99. Peng, S.Y., et al., *HDAC2 Selectively Regulates FOXO3a-Mediated Gene Transcription during Oxidative Stress-Induced Neuronal Cell Death.* Journal of Neuroscience, 2015. **35**(3): p. 1250-1259.

100. Nasrin, N., et al., *DAF-16 recruits the CREB-binding protein coactivator complex to the insulin-like growth factor binding protein 1 promoter in HepG2 cells.* Proceedings of the National Academy of Sciences of the United States of America, 2000. **97**(19): p. 10412-7.

101. Zhang, W.W., et al., *FoxO1 regulates multiple metabolic pathways in the liver - Effects on gluconeogenic, glycolytic, and lipogenic gene expression.* Journal of Biological Chemistry, 2006. **281**(15): p. 10105-10117.

102. Matsumoto, M., et al., *Impaired regulation of hepatic glucose production in mice lacking the forkhead transcription factor foxo1 in liver.* Cell Metabolism, 2007. **6**(3): p. 208-216.

103. Furuyama, T., et al., *Forkhead transcription factor FOXO1 (FKHR)-dependent induction of PDK4 gene expression in skeletal muscle during energy deprivation.* Biochemical Journal, 2003. **375**(Pt 2): p. 365-71.

104. Kamei, Y., et al., *A forkhead transcription factor FKHR up-regulates lipoprotein lipase expression in skeletal muscle.* FEBS Letters, 2003. **536**(1-3): p. 232-6.

105. Bastie, C.C., et al., *FoxO1 stimulates fatty acid uptake and oxidation in muscle cells through CD36-dependent and -independent mechanisms.* Journal of Biological Chemistry, 2005. **280**(14): p. 14222-14229.

106. Tonks, K.T., et al., *Impaired Akt phosphorylation in insulin-resistant human muscle is accompanied by selective and heterogeneous downstream defects.* Diabetologia, 2013. **56**(4): p. 875-885.

107. Milan, G., et al., *Regulation of autophagy and the ubiquitin-proteasome system by the FoxO transcriptional network during muscle atrophy.* Nature Communications, 2015. **6**.

108. O'Neill, B.T., et al., *Insulin and IGF-1 receptors regulate FoxO-mediated signaling in muscle proteostasis.* Journal of Clinical Investigation, 2016. **126**(9): p. 3433-3446.

109. Long, Y.C., et al., *Differential expression of metabolic genes essential for glucose and lipid metabolism in skeletal muscle from spinal cord injured subjects.* Journal of Applied Physiology, 2011. **110**(5): p. 1204-1210.

110. Ouyang, W.M., et al., *An Essential Role of the Forkhead-Box Transcription Factor Foxo1 in Control of T Cell Homeostasis and Tolerance.* Immunity, 2009. **30**(3): p. 358-371.

111. Dengler, H.S., et al., *Distinct functions for the transcription factor Foxo1 at various stages of B cell differentiation.* Nature Immunology, 2008. **9**(12): p. 1388-1398.

112. Lin, L., J.D. Hron, and S.L. Peng, *Regulation of NF-kappaB, Th activation, and autoinflammation by the forkhead transcription factor Foxo3a.* Immunity, 2004. **21**(2): p. 203-13.

113. Cho, J.E., et al., *Time course expression of Foxo transcription factors in skeletal muscle following corticosteroid administration.* Journal of Applied Physiology (1985), 2010. **108**(1): p. 137-45.

114. Hjeltnes, N. *Ryggmärgsskada*. Accessed 2017-11-04.

115. Castro, M.J., et al., *Influence of complete spinal cord injury on skeletal muscle cross-sectional area within the first 6 months of injury.* European Journal of Applied Physiology and Occupational Physiology, 1999. **80**(4): p. 373-378.

116. Shah, P.K., et al., *Lower-extremity muscle cross-sectional area after incomplete spinal cord injury.* Archives of Physical Medicine and Rehabilitation, 2006. **87**(6): p. 772-778.

117. Gorgey, A.S. and G.A. Dudley, *Skeletal muscle atrophy and increased intramuscular fat after incomplete spinal cord injury.* Spinal Cord, 2007. **45**(4): p. 304-9.

118. Elder, C.P., et al., *Intramuscular fat and glucose tolerance after spinal cord injury--a cross-sectional study.* Spinal Cord, 2004. **42**(12): p. 711-6.

119. Talmadge, R.J., et al., *Phenotypic adaptations in human muscle fibers 6 and 24 wk after spinal cord injury.* Journal of Applied Physiology, 2002. **92**(1): p. 147-154.

120. Grimby, G., et al., *Muscle-Fiber Composition in Patients with Traumatic Cord Lesion.* Scandinavian Journal of Rehabilitation Medicine, 1976. **8**(1): p. 37-42.

121. Furuno, K., M.N. Goodman, and A.L. Goldberg, *Role of different proteolytic systems in the degradation of muscle proteins during denervation atrophy.* Journal of Biological Chemistry, 1990. **265**(15): p. 8550-7.

122. Solomon, V. and A.L. Goldberg, *Importance of the ATP-ubiquitin-proteasome pathway in the degradation of soluble and myofibrillar proteins in rabbit muscle extracts.* Journal of Biological Chemistry, 1996. **271**(43): p. 26690-7.

123. Nakae, J., V. Barr, and D. Accili, *Differential regulation of gene expression by insulin and IGF-1 receptors correlates with phosphorylation of a single amino acid residue in the forkhead transcription factor FKHR.* EMBO Journal, 2000. **19**(5): p. 989-96.

124. Seoane, J., et al., *Integration of Smad and forkhead pathways in the control of neuroepithelial and glioblastoma cell proliferation.* Cell, 2004. **117**(2): p. 211-23.

125. Dodd, S., et al., *N-acetylcysteine for antioxidant therapy: pharmacology and clinical utility.* Expert Opinion on Biological Therapy, 2008. **8**(12): p. 1955-62.

126. Mahlapuu, M., et al., *Expression profiling of the gamma-subunit isoforms of AMP-activated protein kinase suggests a major role for gamma3 in white skeletal muscle.* American Journal of Physiology-Endocrinology and Metabolism, 2004. **286**(2): p. E194-200.

127. Gorgey, A.S., et al., *Abundance in proteins expressed after functional electrical stimulation cycling or arm cycling ergometry training in persons with chronic spinal cord injury.* Journal of Spinal Cord Medicine, 2017. **40**(4): p. 439-448.

128. Kwon, O.S., et al., *MyD88 regulates physical inactivity-induced skeletal muscle inflammation, ceramide biosynthesis signaling, and glucose intolerance.* American Journal of Physiology-Endocrinology and Metabolism, 2015. **309**(1): p. E11-E21.

129. Fong, J.H., T.D. Murphy, and K.D. Pruitt, *Comparison of RefSeq protein-coding regions in human and vertebrate genomes.* BMC Genomics, 2013. **14**: p. 654.

130. Dousset, N., et al., *Influence of the environment in space on the biochemical characteristics of human low density lipoproteins.* Free Radical Research, 1996. **24**(1): p. 69-74.